Article:
Senum, S.R., Li, Y.S.M., Benson, K.A. et al. (2022) Monoallelic IFT140 pathogenic variants are an important cause of the autosomal dominant polycystic kidney-spectrum phenotype. The American Journal of Human Genetics, 109 (1). pp. 136-156. ISSN: 0002-9297

https://doi.org/10.1016/j.ajhg.2021.11.016

Monoallelic *IFT140* pathogenic variants are an important cause of the autosomal dominant polycystic kidney-spectrum phenotype

Sarah R. Senum[1], Ying (Sabrina) M. Li[1, 2], Katherine A. Benson[3], Giancarlo Joli[1, 4], Eric Olinger[5], Sravanthi Lavu[1], Charles D. Madsen[1], Adriana V. Gregory[1], Ruxandra Neatu[5], Timothy L. Kline[6], Marie-Pierre Audrézet[7], Patricia Outeda[8], Cherie B. Nau[9], Esther Meijer[10], Hamad Ali[11], Theodore I. Steinman[12], Michal Mrug[13], Paul J. Phelan[14], Terry J. Watnick[8], Dorien J.M. Peters[15], Albert C. M. Ong[16], Peter J. Conlon[17], Ronald D. Perrone[18], Emilie Cornec-Le Gall[7], Marie C. Hogan[1], Vicente E. Torres[1], John A. Sayer[5, 19], Genomics England Research Consortium, the HALT PKD, CRISP, DIPAK, ADPKD Modifier and TAME PKD studies, and Peter C. Harris[1]

[1]Division of Nephrology and Hypertension, [6]Department of Radiology, [9]Department of Ophthalmology, Mayo Clinic, Rochester, MN 55905, USA; [2]Department of Nephrology, Chongqing Municipal Hospital of Traditional Chinese Medicine, Chongqing 400021, China; [3]School of Pharmacy and Biomolecular Science, Royal College of Surgeons in Ireland, Dublin 2, Ireland; [4]University Vita Salute San Raffaele, IRCCS San Raffaele Scientific Institute, 20132 Milan, Italy; [5]Translational and Clinical Research Institute, Faculty of Medical Sciences, Newcastle University, and [19]Renal Services, Newcastle Upon Tyne Hospitals NHS Foundation Trust, and NIHR Newcastle Biomedical Research Centre, Newcastle University, Newcastle upon Tyne, NE4 5PL, UK; [7]Univ Brest, Inserm, UMR 1078, GGB, CHU Brest, F-29200 Brest, France; [8]Division of Nephrology, University of Maryland School of Medicine, Baltimore, MD 21201, USA; [10]Department of Nephrology, University Medical Center Groningen, University of Groningen, 9700 RB Groningen, The Netherlands; [11]Department of Medical Laboratory Sciences, Faculty of Allied Health Sciences, Health Sciences Center, Kuwait University, Sulaibikhat 90805, and Department of Genetics and Bioinformatics, Dasman Diabetes Institute (DDI), Dasman 15462, Kuwait; [12]Renal Division, Beth Israel Deaconess Medical Center, Boston, MA 02215, USA; [13]Division of Nephrology, University of Alabama and the Department of Veterans Affairs Medical Center, Birmingham, AL 35294, USA; [14]Renal Department, NHS Lothian - Royal Infirmary Edinburgh, Edinburgh, EH1 3EG, UK; [15]Department of Human Genetics, Leiden University Medical Center, 2300 RC Leiden, The Netherlands; [16]Kidney Genetics Group, Academic Nephrology Unit, Department of Infection, Immunity and Cardiovascular Disease, University of Sheffield Medical School, and the Sheffield Kidney Institute, Sheffield Teaching Hospitals NHS Foundation Trust, Sheffield, S10 2JF, UK; [17]Department of Nephrology, Beaumont Hospital and Department of Medicine Royal College of Surgeons in Ireland, Dublin 9, Ireland; [18]Division of Nephrology, Tufts Medical Center and Tufts University School of Medicine, Boston, MA 02111, USA.

Corresponding author: Peter C. Harris, Division of Nephrology and Hypertension, Mayo Clinic, Stabile 7, 200 First Street SW, Rochester, MN 55905. Email: harris.peter@mayo.edu

Abstract

Autosomal Dominant Polycystic Kidney Disease (ADPKD), characterized by progressive cyst formation/expansion, results in enlarged kidneys and often end stage kidney disease. ADPKD is genetically heterogeneous; *PKD1* and *PKD2* are the common loci (~78% and ~15% of families) and *GANAB*, *DNAJB11*, and *ALG9* minor genes. PKD is a ciliary associated disease, a ciliopathy, and many syndromic ciliopathies have a PKD phenotype. In a multi-cohort/site collaboration we screened ADPKD diagnosed families that were naïve to genetic testing (n=834) or previously negative from *PKD1* and *PKD2* screening (n=381) employing a PKD targeted next generation sequencing panel (tNGS; n=1186) or whole exome sequencing (WES; n=29). We identified monoallelic loss of function (LoF) variants to *IFT140* in 12 multiplex families and 26 singletons (1.9% of naïve families). IFT140 is a core component of the Intraflagellar transport-complex A, responsible for retrograde ciliary trafficking and ciliary entry of membrane proteins; biallelic *IFT140* variants cause the syndromic ciliopathy, short-rib thoracic dysplasia (SRTD9). The distinctive monoallelic phenotype is mild PKD with large cysts, limited kidney insufficiency, and few liver cysts. Analyses of the Cystic Kidney Disease probands of Genomics England 100K showed that 2.1% had *IFT140* LoF variants. Analysis of the UK Biobank Cystic Kidney Disease group showed probands with *IFT140* LoF variants as the third most common group, after *PKD1* and *PKD2*. The proximity of *IFT140* to *PKD1* (~0.5Mb) in 16p13.3 can cause diagnostic confusion, and *PKD1* variants may modify the IFT140-phenotype. Importantly, our studies link a ciliary structural protein to the ADPKD-spectrum.

INTRODUCTION

Autosomal dominant polycystic kidney disease (ADPKD; MIM: PS173900) is the most common inherited kidney disease, occurring in ~1 in 1000 individuals, and characterized by the progressive development and expansion of kidney cysts, leading to enlarged kidneys and often resulting in end stage kidney disease (ESKD)[1-3]. Frequently found extrarenal manifestations include polycystic liver disease (PLD), that occasionally requires surgical intervention, and intracranial aneurysms that can rupture causing subarachnoid hemorrhage[4; 5]. Approximately 78% and 15% of cases have monoallelic pathogenic variants to *PKD1* (encoding polycystin 1, PC1, MIM: 601313) or *PKD2* (polycystin 2, PC2, MIM: 173910), respectively[6; 7]. PKD1 is a more severe disease with an average age at ESKD of 58.0 years (y) compared to 74.8y for PKD2, with MRI determined total kidney volume (TKV) strongly predicting disease severity[8; 9]. PC1 and PC2 form a receptor complex, and a likely site for this complex associated with PKD is the primary cilium, a sensory antenna found on most cell types[2; 10].

The application of next generation sequencing (NGS), including whole exome sequencing and panels targeting a more limited number of genes (tNGS), to individuals with ADPKD-like phenotypes has identified new loci, including *GANAB* (MIM: 104160), *DNAJB11* (MIM: 611341), and *ALG9* (MIM: 606941), partially accounting for the ~7% of non-PKD1 or -PKD2 families[11-13]. GANAB is rarely associated with ESKD, and can cause autosomal dominant PLD (ADPLD), an ADPKD-related disorder but with few kidney cysts[11; 14]. The implicated protein is glucosidase IIa (GIIa), with its binding partner GIIb (encoded by *PRKCSH*: MIM: 177060), a common cause of ADPLD[15; 16]. In contrast, DNAJB11-nephropathy is characterized by the development of small kidney cysts and fibrosis and resulting in ESKD in later life[12; 17], a phenotype related to autosomal dominant tubulointerstitial kidney disease (ADTKD; MIM: PS162000) due to *UMOD* (MIM:162000) or *MUC1* (MIM: 158340) pathogenic variants[18]. The ALG9 phenotype is of moderate cystic kidney disease and occasional ESKD[13]. *DNAJB11* encodes the endoplasmic reticulum (ER) protein, ERdj3, a co-factor of the chaperone protein BiP, while *ALG9* encodes the ALG9 alpha-1,2-mannosyltransferase. These three gene products are involved in the glycosylation, folding, quality control, and trafficking of membrane and secreted proteins in the ER[19]. Processing of the large, glycosylated membrane protein, PC1, is particularly inhibited by loss or reduction of these ER proteostasis proteins[11-14]. There is also phenotypic overlap between the ADPKD spectrum and ADTKD-*HNF1B* (MIM: 189907) and a number of other monogenic disorders[20-24]. Together these minor loci account for some but not all non-PKD1 or-PKD2 ADPKD-like subjects.

Autosomal recessive PKD (ARPKD) is caused by biallelic pathogenic variants to *PKHD1* (encoding fibrocystin, FPC, MIM: 606702), with the typical phenotype being large echogenic kidneys detected *in*

utero or during infancy with significant neonatal lethality and childhood ESKD, although milder, later childhood or even adult-onset disease can occur[2]. In ARPKD, the liver phenotype is mainly congenital hepatic fibrosis rather than PLD, and single *PKHD1* pathogenic variants have been associated with mild cystic kidney and/or cystic livers[14; 25]. FPC has also been associated with cilia. In addition to these simple kidney and liver focused disorders, a wide range of syndromic diseases associated with cilia, ciliopathies, have kidney and liver phenotypes including the biallelic Meckel syndrome (MKS; MIM: PS249000), Senior-Loken syndrome (SLS; MIM: PS266900), Joubert syndrome (JBTS; MIM: PS213300), short-rib thoracic dysplasia (SRTD; MIM: PS208500), and Bardet-Biedl syndrome (BBS; MIM: PS209900), and the X-linked dominant orofaciodigital syndrome type 1 (OFD1; 311200)[26-28]. The kidney and liver phenotypes include cysts, nephronophthisis (NPHP; MIM: PS256100; tubulointerstitial nephritis and renal fibrosis without kidney enlargement), and congenital hepatic fibrosis. Reflecting the signaling and transporting roles of cilia during development and later, a wide range of additional phenotypes are found in these syndromic ciliopathies. Organ involvement includes the: central nervous system, ranging from encephalocele (MKS), through hypoplasia of the cerebellar vermis (JBTS), to developmental delay (BBS); eye, retinal degeneration manifesting as retinitis pigmentosa or Leber congenital amaurosis (SLS, JBTS, SRTD, BBS); bone, including abdominal skeletal disorders (SRTD), craniofacial abnormalities (SRTD), and polydactyly (MKS, JBTS, SRTD, BBS); and obesity (BBS). At least 70 genes cause syndromic ciliopathies with kidney involvement, with most encoding proteins involved in determining ciliary structure and/or function[29]. These range from proteins involved in intraflagellar transport (IFT), anterograde and retrograde transport systems required to generate the cilium, transport proteins along its length, and for appropriate signaling; transition zone proteins that form a barrier regulating the protein composition of the cilium; and cargo adaptor proteins[28; 30; 31]. The cystic kidney disease associated with these syndromic PKD ciliopathies may be due to reduced polycystin-complex (and/or FPC) in the cilium[32-34], analogous to the ER proteostasis defects causing ADPKD/ADPLD. However, the finding from *in vivo* studies that cilia removal in the kidney in the context of PC1 loss partially rescues PC1 associated cystic disease, questions if there are additional ciliary factors causing or preventing PKD[10; 35].

Here employing NGS of ADPKD-like individuals and analysis of large, sequenced populations, we provide evidence of monoallelic pathogenic variants to a cilia component gene being an important cause of the ADPKD phenotype.

SUBJECTS AND METHODS

Study Participants and Clinical Analysis: Details of the study participants and their recruitment sites are summarized in Figure 1. Subjects were recruited from ADPKD clinical trials: HALT-PKD (n=49)[36; 37], TAME-PKD (n=83)[38] and DIPAK (n=12)[39]; observational ADPKD studies: Consortium for Radiologic Imaging Studies of Polycystic Kidney Disease (CRISP) (n=11)[40] Genkyst (n=10)[41], and DIPAK Observational Study (n=137)[42]; genetic studies of ADPKD: ADKPD Modifier Study (n=49), the Mayo PKD Center (n=737), and the Irish Kidney Gene Project (IKGP; n=35)[43]; and from other academic centers studying ADPKD. The relevant Institutional Review Boards or ethics committees approved all studies, and participants gave informed consent. Clinical and imaging data were obtained by review of clinical records. Hypertension was recorded as the age at which the individual started anti-hypertensive medications or had two or more consecutive readings of 140/90 or above. Kidney volumes were measured by stereology or automatedly[44] from the most recent abdominal CT or MRI and the Mayo Imaging Class (MIC) was determined[8]. Kidney function was calculated as eGFR (mL/min/1.73m^2) from clinical serum creatinine measurements with the Chronic Kidney Disease Epidemiology Collaboration (CKD-EPI) formula[45]. Blood or buccal samples for standard DNA isolation were collected from the probands and all available family members.

Targeted next generation sequencing (tNGS): Screening was performed using either a 137 or 357 gene tNGS panel containing known and candidate PKD and ciliopathy genes[38; 46], and for the 35 IKGP and 69 Brest/Genkyst individuals, as described, respectively, with *IFT140* added to the French panel[17; 43]. As indicated in Figure 1, 352 families were previously negative for pathogenic variants to *PKD1* or *PKD2*, while 834 families had not been previously screened. Library preparation, sequencing, read-alignment, and variant calling were performed as previously described[12; 46]. Variant mining was performed using SNP and Variation Suite (v.8.9.0, Golden Helix; SVS) after employing the following filters: (1) variant-based read depth (DP $\geq$10x) and genotype quality (GQ $\geq$20), (2) removal of variants with minor allele frequency (MAF) >0.01 in GnomAD, and (3) removal of variants >40bp from target coding regions.

Whole exome sequencing (WES): Twenty-nine previously unresolved families were screened by WES at the Mayo Clinic. Genomic DNA (500ng) was sheared by ultrasonication, and libraries were prepared on an Agilent Bravo system using the NEBNext UltraDNA Preparation Kit. Samples were pooled in groups of 12 prior to capture with the Agilent SureSelectXT Human All Exon V7 kit. Samples were sequenced by the Mayo Clinic Genome Analysis Core with 150bp paired-end reads on an Illumina HiSeq4000 with one pool per lane. Read alignment and variant calling was performed using the same methodology as the tNGS panels. Variant mining was done in SVS with the following filters: (1) variant DP $\geq$5x and GQ $\geq$10, (2) removal of variants with MAF >0.001 in GnomAD, and (3) removal of variants >40bp from coding regions.

Sanger screening, copy number variant analysis, and variant assessment and confirmation: Samples where no causative variant was identified in *PKD1* or *PKD2* were further screened using exon specific amplification and Sanger sequencing, with the duplicated region of *PKD1* first amplified by previously described long-range PCR[46]. Large copy number variants (CNV) were assessed from the NGS by calculating the LOG2 ratio of actual read-depth over the expected read-depth for a given locus, and suspected variants confirmed by multiplex ligation-dependent probe amplification (MLPA)[46]. Exon specific PCR primers were designed for confirmation of variants identified in *IFT140* (Table S1) and other genes of interest. Variants of interest in probands and any available family members were confirmed and segregated by amplifying 100ng of gDNA and sequenced bi-directionally at GeneWiz. Ab1 files were analyzed in Mutation Surveyor (V5.1.1, SoftGenetics) to confirm the variant.

The possible significance of missense changes was assessed with the tools: SIFT, Polyphen-2, MutationTaster, MutationAssessor, PROVEAN, FATHMM and CADD, and more broadly as previously described[6; 12; 43]. The pathogenicity of variants was assessed by the American College of Medical Genetic Guidelines (ACMG)[47]. Splicing evaluation was performed using the Berkeley Drosophila Genome Project (BDGP) Splice Site Prediction by Neural Network and Genomnis Human Splice Finder (HSF) sites[48; 49]. Where possible, the phase of *IFT140* and *PKD1* variants was determined by segregation analysis in families.

Genomics England 100K project: All participants in the 100K Genomes Project (100kG) provided written consent to access their anonymized clinical and genomic data for research purposes. The project model and its informed consent process have been approved by the National Research Ethics Service Research Ethics Committee for East of England (Cambridge South Research Ethics Committee). Whole genome sequencing (WGS) was performed using the Illumina TruSeq DNA PCR-Free sample preparation kit (Illumina, Inc.) and an Illumina HiSeq 2500 sequencer, generating a mean depth of 45x (range from 34x to 72x) and greater than 15x for at least 95% of the reference human genome. WGS reads were aligned to the Genome Reference Consortium human genome build 37 (GRCh37) using Isaac Genome Alignment Software (version 01.14; Illumina, Inc.). Sequence data was analyzed using bcftools scripts designed to search vcf.gz files and individual BAM files were viewed using IGV. Variant annotation was performed using Ensembl Variant Effect Predictor (VEP) with the following filter: canonical transcript (ENST00000426508.7), *IFT140* gene and High Impact (see Results for details). Phenotypes of identified carriers were manually reviewed in Genomics England Participant Explorer. Exit Questionnaires, filled in by the clinicians at the NHS Genomics Medical Centres (GMC) for each closed case, have been reviewed

to detect subjects solved for other genes. Those recruited under the "normalized specific disease" term: Cystic Kidney Disease, included 1550 individuals from 1291 families.

UK Biobank: UK Biobank is a large prospective study with over 500,000 participants aged 40–69 years when recruited in 2006–2010 and globally accessible to approved researchers who are undertaking health-related research that's in the public interest[50]. Exome data on ~200,000 individuals have been made available[51]. Ethics approval for the UK Biobank study was obtained from the North West Centre for Research Ethics Committee (11/NW/0382). The exome data of 200,643 individuals was accessed for variants in *IFT140* (GRCh38: chr16:1,510,427-1,612,072) and filtered using Ensembl VEP for High or rare (gnomAD_AF≤0.1%) Low Impact alleles (see Results for details) predicted for the canonical transcript ENST00000426508.7. IMPACT predictions were a subjective classification of the severity of the variant consequence, based on agreement with SNPEff (see also Results). UK biobank diagnoses and disease terms recorded in carriers of High and Low Impact variants were extracted, manually reviewed and filtered for ICD-10 classifiers of kidney disease: Q61.x (Cystic Kidney Disease), N28.1 (Cyst of Kidney), N18.x (Chronic Kidney Disease), N17.x (Acute Renal Failure), I12.x (Hypertensive Renal Disease) and N20.0 (Calculus of Kidney), the term x indicates that all sub-classifications were taken into consideration (e.g., N18.x includes all stages of CKD corresponding to N18.1-N18.5 and N18.9 for unspecified CKD). A Fisher's exact two-sided test was used for enrichment of diagnoses in High Impact variant carriers, and $p \leq 0.05$ considered statistically significant.

The AstraZeneca PheWAS Portal is a repository of gene-phenotype associations for data derived from electronic health records, questionnaires, and continuous traits computed on exomes released by UK Biobank. Gene-level associations were tested using collapsing analyses comparing the proportion of cases with a qualifying variant with the proportion of controls with a qualifying variant in each gene. Twelve different sets of qualifying variant filters (models: 10 dominant models, 1 recessive model and 1 synonymous variant model) were applied to test the association between 18,762 genes and 18,780 phenotypes after extensive quality control filters[52]. Here we analyzed the gene associations with Cystic Kidney Disease (ICD-10 code Q61) using the collapsing model Ptv5pcnt (protein truncating variants; PTV, MAF ≤5% both within the cohort and GnomAD). PTV were designated based on SnpEff annotations and defined as: frameshifting, nonsense, typical splicing, copy number variant, rare missense. Collapsing analysis P values were generated using a Fisher's exact two-sided test. A study-wide significance threshold of $p \leq 2 \times 10^{-9}$ was defined based on an empirical null distribution using the synonymous collapsing model and an n-of-1 permutation-based null distribution.

RESULTS

Study Design: The design of this multinational collaborative study to identify novel genes causative of an ADPKD-like phenotype is shown in Figure 1. Part 1 included screening individuals diagnosed with ADPKD or cystic kidneys, with the vast majority meeting the imaging criteria for ADPKD[53; 54], by tNGS (n=1186) or WES (n=29). Recruitment occurred from 12 different sites or studies, includes subjects negative from previous *PKD1* and *PKD2* sequencing (n=381) and unscreened populations (n=834), with a total of 1215 families screened (see Figure 1 for details). Part 2 of the study included analysis of large populations of individuals that were genetically characterized by WGS, the Cystic Kidney Disease cohort from Genomics England 100K project (100kG; PKD), or WES, the UK Biobank ICD 10 code, Q61: Cystic Kidney Disease (UK Biobank; Q61; Figure 1). One family detected in the 100kG (PKD) project where follow up was possible was analyzed in Part 1 of the project.

***IFT140 is an ADPKD spectrum candidate gene*:** A gene with loss of function (LoF) variants identified in multiple ADPKD families from the tNGS analysis in Part 1 of the study was *IFT140* (MIM: 614620; Chr. 16p13.3). *IFT140* has 29 exons, a coding region of 4386bp (NM_014714.4) and encodes the IFT140 protein of 1462aa (NP_055529.2). IFT140, is a principal component of the IFT-A core complex (along with IFT122 and WDR19 [IFT144]), while IFT43, WDR35 (IFT121) and TTC21B (IFT139) form a peripheral subcomplex[55]. The IFT-A proteins are responsible for dynein-associated retrograde trafficking of proteins from the ciliary tip back to the basal cell body[33; 55-57]. *IFT140* biallelic pathogenic variants have been associated with the syndromic ciliopathy SRTD (SRTD9; MIM 266920), also described as Jeune asphyxiating thoracic dystrophy, Sensenbrenner or Mainzer-Saldino syndromes[58-60]. The SRTD9 phenotype includes retinal dystrophy, skeletal malformations (including small thorax, cone-shaped epiphyses, craniofacial abnormalities, and digit malformations), and chronic kidney disease (cysts and fibrosis)[58; 59]. In addition, biallelic variants to *IFT140* are associated with non-syndromic forms of retinal dystrophy (MIM: 617781), Leber congenital amaurosis and retinitis pigmentosa[61; 62]. Conditional knock-out of *Ift140* in mouse kidney collecting ducts (HoxB7-Cre) demonstrated extensive cystic growth and fibrosis by P20, and short, stumpy cilia[63]. Therefore, *IFT140* was a strong candidate as an ADPKD phenotype gene.

Families with monoallelic IFT140 truncating variants: To determine if *IFT140* variants are causing cystic disease in a monogenic fashion it was important to demonstrate segregation in families. From our screening, 12 multiplex families with two or more members with *IFT140* pathogenic variants and a cystic kidney phenotype were identified, with a total of 40 affected individuals. Clinical details of these families are summarized in Tables 1, S2 and details of the pathogenic *IFT140* variants shown in Table 2.

Pedigree M132: In family M132 PKD was diagnosed in 4 generations, and all tested family members were negative for *PKD1/PKD2* pathogenic variants from Sanger analysis (Figure 2A). The canonical *IFT140* splicing variant c.2399+1G>T was identified simultaneously in an uncle (II-3) and nephew (III-1) by tNGS. Subsequently, the variant was confirmed in III-2 and II-2 was an obligate carrier. A distinctive phenotype of a few, large bilateral kidney cysts but without liver cysts were seen in II-3, III-1, and III-2 (Figure 2B-D), with reduced eGFR seen in III-1. A mild cystic phenotype was also seen in II-1 and IV-1 (Figure 2E, F), and enlarged cystic kidneys described in the grandfather (I-2), but DNA was not available. Of the 7 known and presumed affected members, none experienced ESKD.

Pedigree M199: PKD was diagnosed in 7 individuals over two generations in M199 (Figure 2G). Screening by tNGS identified the *IFT140* frameshifting variant c.2767_2768+2del (p.Tyr923fs*18) in the 4 affected members with DNA available. Kidney imaging was available for 5 individuals, with the disease characterized by a few, larger cysts and in some cases asymmetry between the kidneys, with a single large cyst particularly prominent in III-2 (Figures 2H-K, S1A-C). Four members had renal insufficiency in their 70s, including II-2 with type 2 diabetes who was approaching ESKD when he died at 72y.

Pedigree P1320: The proband, II-1, was diagnosed at 66y with abdominal pain, and ultrasound revealed mild, bilateral kidney cysts and a single liver cyst (Figure 2L, M). Follow up ultrasound and MRI determined that 2 of her 4 children had kidney cysts (Figure 2N), as well one of her sisters (II-2). Screening II-2 by tNGS identified the frameshift variant, *IFT140*: c.2285_2286del (p.Phe762fs*39), that was confirmed in the 3 other affected subjects.

Pedigree EDI1005: The 3 living affected members of this family were screened by WGS as part of the 100kG Project (but where follow up clinical and imaging analysis was possible) and all were found to have the *IFT140* frameshifting variant, c.992_993del (p.Cys331fs*3) (Figure 2O). Follow up imaging analysis revealed large kidneys due to just a few large bilateral cysts, with some kidney asymmetry seen in each individual (Figure 2P-R). The father (I-1) was diagnosed with kidney cysts at 80y and died at 89y without ESKD.

Pedigree 390044: The HALT study proband (III-1) was diagnosed at 41y with a few bilateral kidney cysts, including exophytic cysts (Figure 2S, T). Her mother (II-2) had mild cystic disease, while an aunt (II-1) with PKD had a right kidney nephrectomy at 66y (Figure 2U, V). Genetic analysis of III-1 and II-2 identified the *IFT140* frameshifting variant c.2483delG (p.Gly828fs*18) (DNA was not available from II-1). There was no known prior family history, but the grandparents died in their 50s with limited clinical information available.

Pedigree M1629: The proband, III-2, had multiple bilateral cysts and normal renal function, her father (II-1) had large cysts in both kidneys and declining renal function, and her brother (III-1) mild PKD and normal kidney function (Figures 3A-C, S1D). The typical splicing change, *IFT140*: c.2400-2A>T, was identified or inferred from a linked *PKD1* variant.

Pedigree PK14083: Two siblings (II-1, II-2) had large, bilateral kidneys cysts without liver cysts, and their mother was diagnosed with PKD but died at 92y without ESKD (Figure 3D-F). Both siblings had the *IFT140* frameshift variant c.3696delG (p.Ile1234fs*33).

Pedigree M1554: The mother (II-1) had asymmetric disease with two large left kidney cysts, while the daughter (III-1) has almost unilateral disease with multiple right kidney cysts (Figure 3G-I). Both had normal kidney function and shared the *IFT140* frameshifting variant c.2767_2768+2del.

Pedigree P1497: In this family from the DIPAK randomized clinical trial (RCT), two sisters shared the *IFT140* frameshift variant c.1655_1656del (p.Glu552fs*6); II-1 had multiple large cysts with some asymmetry, and II-2 just a few cysts (Figure 3J-L). Both had normal kidney function, and the family history was uncertain.

Pedigree 1470059: In this family from the ADPKD Modifier study, the proband (II-1) had large cystic kidneys with a few large cysts and renal insufficiency at 76y, while his son (III-1) has just a few tiny bilateral cysts (Figure 3M-O). *IFT140* c.1655_1656del segregated in these individuals.

Pedigree M1169: The proband in this family (II-1) had mild bilateral renal cystic disease and no liver cysts (Figure 3P, Q). Her father (I-1) had 2 left kidney cysts and shared the nonsense variant *IFT140*: c.1377G>A (p.Trp459*) with II-1. The sister II-2 was reported to have bilateral kidney cysts but limited clinical information and no DNA was available (Table S2).

Pedigree M1266: The proband, II-2, had multiple small kidney cysts, some exophytic, and multiple small liver cysts (Figure 3R-S), while her sister (II-1) had multiple small kidney cysts, with one larger cyst. Both shared the *IFT140* frameshift variant, c.223delG (p.Val75fs*11).

Singleton individuals with monoallelic IFT140 truncating variants: In addition to the multiplex families, 26 families with a single genetically and clinically confirmed case with an *IFT140* pathogenic variant were identified (see Tables 1, 2 and Figures S1-S3 for details). The majority of these families did not have a known family history, but in 7 families an affected relative was known or suspected but a sample to test segregation and detailed clinical data was not available (Table S2). In pedigree F392 two relatives had the familial *IFT140* variant but had negative ultrasounds at 53y and 40y, and in M241 the son had the family variant, but no clinical information was available. The phenotype in the singleton subjects was consistent with the familial cases; the kidney disease was generally bilateral with variable numbers of large cysts present and few liver cysts (Figures S1-S3). Unlike the multiplex families where all variants were

truncating, 4 singleton cases had non-truncating variants. Two were larger inframe deletions that scored as likely pathogenic by ACMG guidelines (Figure S3G, I) and two were missense changes that have previously been scored as likely pathogenic changes associated with SRTD9; including c.634G>A (p.Gly212?) that is a likely splicing variant (Figure S3B, C, E; Table 2).

IFT140 pathogenic variants are strongly enriched in cystic kidney families*:* Our analysis identified 38 families with *IFT140* pathogenic variants, 36 from tNGS and 1 from WES, plus one from WGS (Figure 1). None of these families had a LoF *PKD1* or *PKD2* (or other ADPKD-like gene) variant. Of the previously unscreened families, 16/834 (1.9%) had an *IFT140* pathogenic variant. This compared to 21/381 (5.5%) of previously *PKD1* and *PKD2* negative families (Figure 1).

Genomics England 100k Genomes Project analysis*:* To determine the burden of likely pathogenic *IFT140* variants more broadly we analyzed genetic and clinical data from the 100k Genomes Project that includes National Health Service (NHS) subjects affected by a rare disease or cancer, plus relatives. *IFT140* variants were extracted from WGS of 64,185 subjects and after annotation 26 distinct strongly predicted pathogenic variants (stop gain, start loss, and canonical splice acceptor and donor variants) were identified in a total of 152 individuals (89 probands and 63 relatives) from 111 different families. Among these 152 individuals, kidney cyst(s) were described in 40 individuals (26.3%), including 31/89 probands (34.8%); 27 of these probands were recruited to the 100kG under the "Cystic Kidney Disease" (100kG; PKD) group. Analysis of the 100kG; PKD group showed that 27/1291 (2.1%) probands had *IFT140* likely pathogenic variants, but these variants were much rarer in probands in other rare disease groups (62/33,127; 0.19%; $p<0.0001$) or probands with primary neurological diagnoses (18/8,162; 0.22%; $p<0.0001$). Twenty-five IFT140 positive probands in the 100kG; PKD group were considered unsolved by the Genomics England analysis; 2 carried monoallelic VUS in *PKD1* (see Tables 3, and S2). Three families showed segregation of the *IFT140* variant with the cystic phenotype in 3, 2 or 1 family member (Table S3).

UK Biobank analysis: Recently *IFT140,* or the recurrent *IFT140* LoF variant c.2399+1G>T, were suggested associated with kidney cyst phenotypes in the UK Biobank population and the TOPMed Program[52; 64]. UK Biobank subjects were typically between 50-75y, and the study was not enriched for monogenic disease. A total of 240,037 individuals with WES data were available for study[52]. Genes were screened for enrichment of protein truncating variants (including nonsense, canonical splice, or frameshifts) in the ICD-10 code Q61 (Cystic Kidney Disease; n=521) group compared to controls (without Q61; n=239,516). Individuals with monoallelic *IFT140* truncating variants represented 2.69% of Q61 cases compared to 0.21% of controls (-log10 $p=1.62e^{-11}$; Figure 4A). Carriers of truncating variants to *PKD1*, 8.45% cases vs. 0.015% controls and *PKD2*, 5.57% cases vs. 0.004% were also, as expected, highly enriched in the PKD

group (-log 10 p=3.04e^{-96} and 1.63e^{-69}, respectively). *ALG9* truncating variant carriers, 0.77% cases and 0.032% controls, were the next highest but not significantly enriched (-log10 p=000030; significance threshold p=1.0e$^{-8.7}$).

In a separate analysis of the UK Biobank population, the prevalence of High (likely pathogenic: frameshifting, nonsense, or canonical splicing) vs. Low Impact variants (likely benign: synonymous, non-canonical intronic) with a gnomAD minor allele frequency ≤0.1% were compared for various ICD-10 kidney disease codes (Figure 4B). For this analysis, out of a total population of 200,643 subjects with WES data, 481 individuals were monoallelic for High and 5,888 had Low Impact *IFT140* variants. ICD-10 codes for Cyst of Kidney (N28.1), Cystic Kidney Disease (Q61), and CKD stages 4&5 (N18.4 & N18.5) were more common in individuals carrying High compared to Low Impact *IFT140* variants: 2.7% vs 0.5% (P=1.3x10^{-5}, OR=5.3; 95CI: 2.7-10.1); 1.0% vs 0.07% (P=2.4x10^{-4}, OR=15.4; 95CI 4.7-50.5) and 1.0% vs 0.3% (P=0.02, OR=3.9; 95CI 1.5-10.3), respectively, whereas other kidney phenotypes were not significant (Figure 4B).

The monoallelic IFT140 phenotype: IFT140 subjects from Part 1 of the study typically had conserved renal function, but 32 had an eGFR <60, and one with a single kidney due to nephrectomy following infantile Wilms tumor had ESKD at 64y (Table 1, S2). A plot of eGFR versus age showed an overall milder disease course than for PKD2 but a lower eGFR than seen in normal individuals (Figure 5A)[65]. IFT140 individuals were diagnosed at a mean age of 52.7y (± 13.2y), compared to 29.9y (± 11.9y) for the ADPKD individuals in the TAME study[66], and the diagnosis was often made incidentally. Hypertension was diagnosed in 66.1% of individuals (where the information was available), with an average age at onset of 56.9y (the precise age at onset was not present in 14 individuals, and the mean eliminating those was 53.6y); only one affected individual was hypertensive before 40y. Therefore, hypertension was less frequent and diagnosed approximately 20 years later than in ADPKD overall[67]. Six IFT140 individuals had a vascular phenotype, including intracranial or aortic aneurysm, and some of these individuals had additional PKD gene variants (Table 3), but further study will be required to see if there is an association as found in ADPKD overall[4; 5]. The htTKV was often enlarged in the monoallelic *IFTI40* subjects but asymmetry was common with a small number of cysts accounting for most of the cystic disease (and increased TKV), hence, 27 individuals were classified as having an atypical (2A) MIC[8]. Plotting the htTKV data shows a wide spread of values both for those with a typical and atypical MIC (Figure 5B). Liver cysts were rare, found in only 9 subjects, and when present were usually small (Table 1).

Retinal degeneration is a phenotype associated with biallelic *IFT140* pathogenic variants and there was some anecdotal analysis of eye disease in monoallelic individuals. M199: III-1 had age-related macular degeneration (AMD) and early-stage retinal pigment epithelium (RPE) detachment, while M1374: R3376

had AMD and atrophy of the RPE (Table S2; Figure S4). In addition, P1505: Ox5262 had congenital aniridia and blindness (see also below). However, only a limited number of eye exams were available and analyses in these individuals by an optometrist revealed no systematic eye phenotype. In addition, several individuals had a diagnosis of cancer, including 5 with colorectal cancer but further analysis will be required to determine if there is any association. Of note in the 100kG data, 9 High Impact *IFT140* variant carriers had diaphragmatic (or umbilical) hernias, 7 of whom also had kidney cysts, while in the UK Biobank data, ICD-10 K40.9 (unilateral or unspecified inguinal hernia, without obstruction or gangrene) was enriched in High Impact carriers (p=0.016).

Genetic variants in other genes: *IFT140* lies in chromosome region 16p13.3 (16: 1560428-1662111; hg19) less than 0.5Mb distal to *PKD1* (16: 2138711-2185899; hg19). Consequently by linkage analysis, *IFT140* pathogenic variants can be linked to *PKD1* variants in family and sometimes population analyses. For instance, 3 families with *IFT140*: c.2399+1G>T also had the *PKD1* variant c.11017-3C>T; these variants co-segregated with the disease in M132 (Figure 2A, Table 3). This *PKD1* noncanonical splicing change has been described as pathogenic but is not predicted to significantly alter splicing and is found 298 times in gnomAD[68]. As another example, *PKD1*: c.2990C>T (p.Thr997Met), a somewhat conservative substitution at a residue well conserved in *PKD1* orthologs, but not in the PKD Repeat domain, and found twice in gnomAD, was considered pathogenic from clinical testing because it segregated in 3 affected individuals in M1629, but *IFT140*: c.2400-2A>T also segregates in this family (Figure 3A). Variants of possible significance in other PKD genes were also found in IFT140 families. For instance, M1266 has the *PKHD1* frameshifting variant c.3549delT (p.His1184fs*36), as well as *IFT140*: c.223delG, both segregating in the two affected sisters and perhaps associated with the liver cysts. Families P1504 and F662 had a LoF variant in another IFT-A encoding gene, *IFT43* (MIM: 614068) or *TTC21B* (MIM: 612014), respectively, and R1403 (M241) had a single LoF to the SRTD gene, *WDR60* (MIM: 615462). LoF variants in 3 other ciliopathy genes were found in 3 other families (Table 3), but some variants, *BBS2* (MIM: 606151): c. 823C>T (p.Arg275*) (M1320; Figure 2L) and *DYNC2H1* (MIM: 603297): c.3054delC (p.Phe1018fs*3) (M199; Figure 2G), did not fully segregate with the disease. P1505 had the *OFD1* (MIM: 300171) canonical splicing variant c.936-2A>G, but which is present 24 times in gnomAD and the significance is uncertain. The eye phenotype in this family could be associated with the *IFT140* and/or *OFD1* variants.

DISCUSSION

We provide overwhelming evidence that monoallelic *IFT140* LoF variants cause an ADPKD-like phenotype. Given the phenotypic and genotypic variability associated with monoallelic causes of cystic kidney disease

(*PKD1, PKD2, GANAB, DNAJB11, ALG9, etc.*), and the familiarity with the ADPKD term by nephrologists and affected individuals, we suggest calling this group of disorders the ADPKD-spectrum, and adding the affected gene as a suffix to better describe the disease (i.e. ADPKD-*PKD1* or ADPKD-*IFT140*)[7]. Our data comes from family-based and population studies. The families include 12 multiplex pedigrees, where segregation was demonstrated or inferred in 33 family members with 7 other likely affected family members, and in 26 singletons, 7 of whom had relatives with kidney cysts. In total, ADPKD-*IFT140* represented 1.9% of naïve screened families and 5.5% of those previously negative for *PKD1* or *PKD2* pathogenic variants, with c.2399+1G>T a relatively common pathogenic variant. WES as well as tNGS was employed for screening, and no ADPKD-*IFT140* families had LoF variants to *PKD1*, *PKD2* or other ADPKD-spectrum genes. Of note, families were identified in clinical trials (HALT PKD, DIPAK RCT, and TAME) and observational studies (CRISP, ADPKD Modifier, Genkyst, DIPAK Observational), where a clinical diagnosis of ADPKD was required for recruitment. In one family, 2 individuals had the familial *IFT140* pathogenic variant, but kidney cysts were not detected. However, only abdominal ultrasound imaging was available that has lower resolution than MRI or CT. The negative imaging likely reflects the reduced penetrance of ADPKD-*IFT140* compared to ADPKD-*PKD1* or ADPKD-*PKD2*, similar to the ADPLD genes where affected individuals may live to old age without a diagnosis unless appropriate imaging is performed[69].

The population data, both from the 100kG; PKD cohort and UK Biobank, support I*FT140* as a significant ADPKD-spectrum gene. *IFT140* accounted for 2.1% of the 100kG; PKD cohort, none of which had LoF *PKD1* or PKD2 variants. In the UK Biobank ICD-10 code Q61 Cystic Kidney Disease cohort *IFT140* was identified as the 3rd most enriched ADPKD-spectrum gene. Due to the recruitment criteria, this cohort is likely enriched for milder PKD subjects, but nevertheless, no other gene apart from *PKD1* and *PKD2* was significantly associated with this group. This is consistent with the larger number of identified IFT140 pedigrees described here than for any other ADPKD-spectrum gene, apart from *PKD1* and *PKD2*[11-14; 17; 22; 70-73]. The phenotype is also very consistent, reflective of a monogenic disease; a few large kidney cysts resulting in increased htTKV, renal insufficiency just in older individuals but rarely ESKD, and liver cysts rare or not present. Nevertheless, UK Biobank participants with *IFT140* LoF variants were enriched for CKD4 & 5, indicating that it is not an entirely benign phenotype.

Although monoallelic *IFT140* pathogenic variants rarely cause ESKD, defining this ADPKD-spectrum gene is important for diagnostics and prognostics. This diagnosis can differentiate a family from ones with *PKD1*, *PKD2* or *DNAJB11* variants, where the chance of ESKD is much greater. Therefore, an IFT140 diagnosis may be reassuring, although if extrarenal phenotypes are associated with *IFT140* haploinsufficiency needs further study in larger populations and 100kG and UK Biobank data. The

significant number of IFT140 individuals with additional variants to *PKD1, PKHD1,* or other ciliopathy genes emphasizes that the IFT140-phenotype may be modified by coinheritance of variants in these other cystogenes. Along with reduced penetrance, genetic modification may explain some of the intrafamilial phenotypic variability. Animal studies and human observations indicate that variants in more than one PKD/PLD gene can combine to accentuate the phenotype[74-78]. Given the close localization of *IFT140* and *PKD1* in 16p13.3, a *PKD1* modifying variant may co-segregate in multiple affected individuals, and *PKD1* analysis alone may misdiagnose the modifying variant as disease causing. Therefore, screening *IFT140* along with *PKD1* and other ADPKD-spectrum genes is important to achieve an accurate molecular diagnosis. The mild phenotype and likely effect of disease modifiers may explain why ADPKD-*IFT140* has hitherto remained unrecognized. Population studies by imaging have identified quite large populations with probable and possible ADPKD, that may partly be accounted for by *IFT140* variants[3]. Interestingly in the UK Biobank, *IFT140* LoF variants were associated with ICD-10 code N-28.1, Cyst of Kidney. This code includes a small number of "simple" cysts or supposed acquired cystic disease, but our work indicates that some of this group have a monogenic cause.

Kidney size, categorized by htTKV/age into 5 typical MIC (A-E), is a strong predictor of future decline in renal function in ADPKD[8; 9]. For some ADPKD-spectrum genes, such as *DNAJB11*, ESKD can occur without kidney enlargement due to fibrosis; many affected individuals have the atypical, atrophic MIC, 2B, and htTKV/age is not a good predictor of future kidney function[17]. ADPKD-*IFT140* individuals often have enlarged kidneys due to a few large cysts, sometimes resulting in asymmetry and often being categorized as an atypical presentation due to just a few cysts accounting for a large proportion of the TKV (MIC, 2A). However, even if the individual is assigned to a typical MIC, because of the enlargement due to a few large cysts and likely preserved parenchyma, the MIC is not predictive of future renal insufficiency. For ADPKD-spectrum genes, especially beyond *PKD1* and *PKD2*, the addition of genetic data better allows the interpretation of imaging results[9].

As seen for *IFT140*, there are precedents for biallelic disruption of ADPKD-spectrum genes being associated with viable but more severe phenotypes, including kidney cysts. Biallelic pathogenic variants to *PKD1* and probably *PKD2*, where at least one variant is hypomorphic, can be associated with very early onset PKD, similar to ARPKD[79-81]. Monoallelic *PKHD1* pathogenic variants can be associated with mild PKD/PLD, and recently biallelic *DNAJB11* variants have been associated with an ARPKD-like disease with pancreatic cysts[14; 25; 82; 83]. Biallelic variants to *ALG9*, or the ADPLD-associated *ALG8* (MIM: 608103), cause congenital defects of glycosylation (CDG1L and CDG1H, respectively), that involve cystic kidneys as part of severe, developmental disorders[84; 85]. In many of these disorders, including the association of biallelic

IFT140 variants with SRTD, two LoF variants are probably not compatible with life (viable individuals have at least one nontruncating variant)[58; 59; 86-88]. It therefore follows that these ADPKD-spectrum subjects are unusually vulnerablity to cyst development from ADPKD gene dosage reduction.

There has long been rigorous debate about the mechanism of disease in ADPKD, with just a single germline mutation required for cysts development. The detection of somatic mutations to the germline gene in cyst linings, and that induced loss of *Pkd1* or *Pkd2* in the kidney results in cyst development, support a two-hit model of cyst initiation[89-91]. However, biallelic disease, that cysts can develop when PC1 is present, and the link between severity of kidney disease and the level of functional PC1, suggest a dosage/threshold model of cystogenesis[88; 92-94]. The mechanism of cyst development associated with monoallelic *IFT140* pathogenic variants is not known, but the small number of cysts present could be compatible with a two-hit model. Interestingly, larger deletion somatic events (loss of heterozygosity; LOH) may also delete *PKD1*, resulting in a dosage loss that may further promote cyst development/expansion. Likewise, *PKD1* somatic LOH may include deletion of an *IFT140* allele[95]. However, since the tuberous sclerosis gene, *TSC2* (MIM: 191092), lies between *PKD1* and *IFT140,* germline deletions including both genes would result in the more rapidly progressive cystic disease plus TSC phenotypes of the *PKD1-TSC2* contiguous gene syndrome[96; 97].

The described minor ADPKD-spectrum and most ADPLD proteins are involved in protein folding and trafficking in the ER, with PC1 an identified protein particularly sensitive to dosage reduction of these proteins resulting in reduced surface and ciliary localization of the PC-complex[11-14; 76]. However, here we implicate a protein involved in ciliary structure and function as an ADPKD-spectrum gene. This is important because although loss or disruption of ciliary function has been associated with a cystic phenotype, as part of a syndromic ciliopathy phenotype or in experimental models, in monoallelic human disease it has not been directly shown to cause cyst formation. Indeed, there has been debate whether additional cystogenic factors other than the PC complex and FPC promote cyst formation and/or the NPHP phenotype[10]. The cystogenic effect of *IFT140* haploinsufficiency also seems unusual, since although other IFT-A or SRTD genes were found as modifiers (Table 3), our screening did not indicate any as common monoallelic causes of the ADPKD-spectrum.

It is not known if a 50% dosage reduction of IFT140 results in changes in ciliary structure/function, but the documented null phenotype is greatly shortened cilia with a bulbous tip, illustrating its role in retrograde IFT[63]. However, the IFT-A complex has also been implicated in the regulation of protein localization and gating of the ciliary transition zone during ciliary assembly[33; 56; 57]. In human cells, loss of the core IFT-A complex protein WDR19 (IFT144) results in failed ciliary entry of the IFT-A complex and

membrane proteins and accumulation of IFT-B complex proteins at the bulbous tip[55]. In Chlamydomonas, analysis of truncated IFT140, missing the critical WD repeats, demonstrated improper localization of multiple membrane-bound ciliary proteins[57]. While in *C. elegans*, IFT140 has a role in restricting entry of ciliary membrane proteins, whereas the peripheral IFT-A proteins have been implicated in protein removal from cilia[56]. Since PC1, PC2 and FPC are ciliary localized membrane cystoproteins, and the trafficked level of PC1, at least, seems critical for preventing cystogenesis, subtle reductions of ciliary entry of PC1 (and PC2 and FPC) may underlie cyst development in monoallelic IFT140 subjects. However, further structural and functional analysis of IFT140$^{+/-}$ cilia is required to better understand cystogenesis in this setting.

In conclusion, monoallelic LoF *IFT140* variants result in an atypical, mild form of ADPKD, consisting of large bilateral cysts and renal functional decline in older ages. *IFT140* likely represents >1% of ADPKD-spectrum individuals and is found in many studied ADPKD cohorts. Association of an IFT-complex protein with the ADPKD-spectrum strengthens the link between ciliary defects and ADPKD, and may help understand pathogenesis in the wider group of ADPKD-spectrum disorders.

DESCRIPTION OF SUPPLEMENTAL DATA

Table S1: Primer sets for *IFT140* variant confirmation and segregation.

Table S2: Genetic and other phenotypic details of individuals with *IFT140* pathogenic variants

Table S3: Details of individuals with *IFT140* pathogenic variants in the 100K Genomes Cystic Kidney Disease Cohort.

Figure S1. Ultrasound images of IFT140 subjects' kidneys.

Figure S2: Kidney and liver images of 16 singleton subjects with *IFT140* pathogenic variants.

Figure S3: Genetic and phenotypic details of individuals with inframe *IFT140* pathogenic variants.

Figure S4: Optical Coherence Tomography imaging of ocular phenotypes in two *IFT140* LoF subjects.

Acknowledgement of associated consortium members.

DECLARATION OF INTERESTS

MM reports grants and consulting fees outside the submitted work from Otsuka Pharmaceuticals, Sanofi, Chinook, Goldilocks, Natera, and Palladio. RDP reports clinical trial support from Reata, Kadmon, Sanofi-Genzyme, US Dept. of Defense, consultant/advisory fees from Otsuka, Sanofi-Genzyme and is Section editor Renal Cystic Disease: UpToDate. JAS has received honorarium from consulting positions from Otsuka Pharmaceuticals, Sanofi, and Takeda. VET reports grants and/or other fees from Mironid, Blueprint Medicines, Otsuka Pharmaceuticals, Palladio Biosciences, Sanofi Genzyme, Reata, and Regulus Therapeutics, all outside the submitted work.

ACKNOWLEDGEMENTS

We thank the families and coordinators for involvement in the study, and Saurabh Baheti (Mayo Clinic), Dana Miskulin (Tufts University), Susan L Murray (Beaumont Hospital, Dublin) Aurore Despres and Christelle Guillerm (CHU Brest), Aude Promerat and Cécile Lemoine (Roubaix), Anne-Laure Faucon (Corbeil-Essone), Emad Khazned (Bourges), Alain Michel (Saint Malo), Charles J Blijdorp (Erasmus Medical Center, Rotterdam), Rene MM van Aerts (University Medical Center Radboud, Nijmegen) Shosha EI Dekker (Leiden University Medical Center) for technical assistance or referring individuals. This research was conducted using data from UK Biobank (project ID 43879; www.ukbiobank.ac.uk) and data and findings from the 100,000 Genomes Project.

The study was supported by NIDDK grants DK058816 and DK059597 (PCH), the Mayo Translational PKD Center (DK090728; VET), the Zell Family Foundation, Robert and Billie Kelley Pirnie, an Early Postdoc Mobility Stipendium, Swiss National Science Foundation (P2ZHP3_195181) and Kidney Research UK (Paed_RP_001_20180925) (EO), Kidney Research UK and the Northern Counties Kidney Research Fund (JAS), a Barbour Foundation Postgraduate Research Studentship (RP), and Kuwait Foundation for the Advancement of Sciences (KFAS) grant PR17-13MM-07 (HO). The Irish Kidney Gene Project was funded by the Health Research Board, Irish Nephrology Society, Irish Kidney Association under the HRCI-HRB Joint Funding Scheme HRCI-HRB-2020-032, the Baltimore PKD Research and Clinical Core Center were supported by P30DK090868 and U54 DK126114.

Support for HALT PKD, CRISP, the ADPKD Modifier Study, Genkyst, DIPAK, the UK Biobank, and the 100,000 Genomes Project are shown in the Supplemental Material, along with additional investigators from these studies.

WEB RESOURCES

ACMG Calculator, https://www.medschool.umaryland.edu/genetic_variant_interpretation_tool1.html/

ADPKD Mutation Database (PKD DB), http://pkdb.mayo.edu

AstraZeneca PheWAS Portal, https://azphewas.com/

ClinVar, https://www.ncbi.nlm.nih.gov/clinvar/

Ensembl Genome Browser, https://useast.ensembl.org/index.html

GnomAD Browser, http://gnomad.broadinstitute.org/

Genomics England 100K Project, https://www.genomicsengland.co.uk/

IMPACT predictions, Ensembl Variation - Calculated variant consequences, https://www.ensembl.org/info/genome/variation/prediction/predicted_data.html

Mayo Imaging Class, https://www.mayo.edu/research/documents/pkd-center-adpkd-classification/doc-20094754

NCBI Nucleotide, http://www.ncbi.nlm.nih.gov/nuccore

OMIM, http://www.omim.org

RefSeq, http://www.ncbi.nlm.nih.gov/refseq/

SnpEff variant annotations, http://pcingola.github.io/SnpEff/

UCSC Genome Browser, https://genome.ucsc.edu

UK Biobank, https://www.ukbiobank.ac.uk/

UK Biobank showcase portal, https://biobank.ndph.ox.ac.uk/showcase/label. cgi?id=170

DATA AND CODE AVAILABILITY

Primary data from the 100,000 Genomes Project, which are held in a secure research environment, are available to registered users.

UK biobank association statistics are publicly available through the AstraZeneca Centre for Genomics Research (CGR) PheWAS Portal. All whole-exome sequencing data described in this paper are publicly available to registered researchers through the UKB data access protocol.

REFERENCES

1. Cornec-Le Gall, E., Alam, A., and Perrone, R.D. (2019). Autosomal dominant polycystic kidney disease. Lancet. 393, 919-935.
2. Bergmann, C., Guay-Woodford, L.M., Harris, P.C., Horie, S., Peters, D.J.M., and Torres, V.E. (2018). Polycystic kidney disease. Nat Rev Dis Primers. 4, 50.
3. Suwabe, T., Shukoor, S., Chamberlain, A.M., Killian, J.M., King, B.F., Edwards, M., Senum, S.R., Madsen, C.D., Chebib, F.T., Hogan, M.C., et al. (2020). Epidemiology of Autosomal Dominant Polycystic Kidney Disease in Olmsted County. Clin J Am Soc Nephrol. 15, 69-79.
4. Hogan, M.C., Abebe, K., Torres, V.E., Chapman, A.B., Bae, K.T., Tao, C., Sun, H., Perrone, R.D., Steinman, T.I., Braun, W., et al. (2015). Liver Involvement in Early Autosomal-Dominant Polycystic Kidney Disease. Clin Gastroenterol Hepatol. 13, 155-164.
5. Sanchis, I.M., Shukoor, S., Irazabal, M.V., Madsen, C.D., Chebib, F.T., Hogan, M.C., El-Zoghby, Z., Harris, P.C., Huston, J., Brown, R.D., et al. (2019). Presymptomatic Screening for Intracranial Aneurysms in Patients with Autosomal Dominant Polycystic Kidney Disease. Clin J Am Soc Nephrol. 14, 1151-1160.
6. Heyer, C.M., Sundsbak, J.L., Abebe, K.Z., Chapman, A.B., Torres, V.E., Grantham, J.J., Bae, K.T., Schrier, R.W., Perrone, R.D., Braun, W.E., et al. (2016). Predicted Mutation Strength of Nontruncating PKD1 Mutations Aids Genotype-Phenotype Correlations in Autosomal Dominant Polycystic Kidney Disease. J Am Soc Nephrol. 27, 2872-2884.
7. Cornec-Le Gall, E., Torres, V.E., and Harris, P.C. (2018). Genetic Complexity of Autosomal Dominant Polycystic Kidney and Liver Diseases. J Am Soc Nephrol. 29, 13-23.
8. Irazabal, M.V., Rangel, L.J., Bergstralh, E.J., Osborn, S.L., Harmon, A.J., Sundsbak, J.L., Bae, K.T., Chapman, A.B., Grantham, J.J., Mrug, M., et al. (2015). Imaging classification of autosomal dominant polycystic kidney disease: a simple model for selecting patients for clinical trials. J Am Soc Nephrol. 26, 160-172.
9. Lavu, S., Vaughan, L.E., Senum, S.R., Kline, T.L., Chapman, A.B., Perrone, R.D., Mrug, M., Braun, W.E., Steinman, T.I., Rahbari-Oskoui, F.F., et al. (2020). The value of genotypic and imaging information to predict functional and structural outcomes in ADPKD. JCI Insight. 5, e138724.
10. Ma, M., Gallagher, A.R., and Somlo, S. (2017). Ciliary Mechanisms of Cyst Formation in Polycystic Kidney Disease. Cold Spring Harb Perspect Biol. 9, a028209.
11. Porath, B., Gainullin, V.G., Cornec-Le Gall, E., Dillinger, E.K., Heyer, C.M., Hopp, K., Edwards, M.E., Madsen, C.D., Mauritz, S.R., Banks, C.J., et al. (2016). Mutations in GANAB, Encoding the Glucosidase IIalpha Subunit, Cause Autosomal-Dominant Polycystic Kidney and Liver Disease. Am J Hum Genet. 98, 1193-1207.
12. Cornec-Le Gall, E., Olson, R.J., Besse, W., Heyer, C.M., Gainullin, V.G., Smith, J.M., Audrezet, M.P., Hopp, K., Porath, B., Shi, B., et al. (2018). Monoallelic Mutations to DNAJB11 Cause Atypical Autosomal-Dominant Polycystic Kidney Disease. Am J Hum Genet. 102, 832-844.

13. Besse, W., Chang, A.R., Luo, J.Z., Triffo, W.J., Moore, B.S., Gulati, A., Hartzel, D.N., Mane, S., Regeneron Genetics, C., Torres, V.E., et al. (2019). ALG9 Mutation Carriers Develop Kidney and Liver Cysts. J Am Soc Nephrol. 30, 2091-2102.
14. Besse, W., Dong, K., Choi, J., Punia, S., Fedeles, S.V., Choi, M., Gallagher, A.R., Huang, E.B., Gulati, A., Knight, J., et al. (2017). Isolated polycystic liver disease genes define effectors of polycystin-1 function. J Clin Invest. 127, 1772-1785.
15. Drenth, J.P., te Morsche, R.H., Smink, R., Bonifacino, J.S., and Jansen, J.B. (2003). Germline mutations in *PRKCSH* are associated with autosomal dominant polycystic liver disease. Nat Genet. 33, 345-347.
16. Li, A., Davila, S., Furu, L., Qian, Q., Tian, X., Kamath, P.S., King, B.F., Torres, V.E., and Somlo, S. (2003). Mutations in PRKCSH cause isolated autosomal dominant polycystic liver disease. Am J Hum Genet. 72, 691-703.
17. Huynh, V.T., Audrezet, M.P., Sayer, J.A., Ong, A.C., Lefevre, S., Le Brun, V., Despres, A., Senum, S.R., Chebib, F.T., Barroso-Gil, M., et al. (2020). Clinical spectrum, prognosis and estimated prevalence of DNAJB11-kidney disease. Kidney Int. 98, 476-487.
18. Devuyst, O., Olinger, E., Weber, S., Eckardt, K.U., Kmoch, S., Rampoldi, L., and Bleyer, A.J. (2019). Autosomal dominant tubulointerstitial kidney disease. Nat Rev Dis Primers. 5, 60.
19. Hu, J., and Harris, P.C. (2020). Regulation of polycystin expression, maturation and trafficking. Cell Signal. 72, 109630.
20. Izzi, C., Dordoni, C., Econimo, L., Delbarba, E., Grati, F.R., Martin, E., Mazza, C., Savoldi, G., Rampoldi, L., Alberici, F., et al. (2020). Variable Expressivity of HNF1B Nephropathy, From Renal Cysts and Diabetes to Medullary Sponge Kidney Through Tubulo-interstitial Kidney Disease. Kidney Int Rep. 5, 2341-2350.
21. Gulati, A., Bae, K.T., Somlo, S., and Watnick, T. (2018). Genomic Analysis to Avoid Misdiagnosis of Adults With Bilateral Renal Cysts. Ann Intern Med. 169, 130-131.
22. Schönauer, R., Baatz, S., Nemitz-Kliemchen, M., Frank, V., Petzold, F., Sewerin, S., Popp, B., Münch, J., Neuber, S., Bergmann, C., et al. (2020). Matching clinical and genetic diagnoses in autosomal dominant polycystic kidney disease reveals novel phenocopies and potential candidate genes. Genet Med. 22, 1374-1383.
23. Gulati, A., Sevillano, A.M., Praga, M., Gutierrez, E., Alba, I., Dahl, N.K., Besse, W., Choi, J., and Somlo, S. (2020). Collagen IV Gene Mutations in Adults With Bilateral Renal Cysts and CKD. Kidney Int Rep. 5, 103-108.
24. Cornec-Le Gall, E., Chebib, F.T., Madsen, C.D., Senum, S.R., Heyer, C.M., Lanpher, B.C., Patterson, M.C., Albright, R.C., Yu, A.S., Torres, V.E., et al. (2018). The Value of Genetic Testing in Polycystic Kidney Diseases Illustrated by a Family With PKD2 and COL4A1 Mutations. Am J Kidney Dis. 72, 302-308.
25. Gunay-Aygun, M., Turkbey, B.I., Bryant, J., Daryanani, K.T., Gerstein, M.T., Piwnica-Worms, K., Choyke, P., Heller, T., and Gahl, W.A. (2011). Hepatorenal findings in obligate heterozygotes for autosomal recessive polycystic kidney disease. Mol Genet Metab. 104, 677-681.
26. Hildebrandt, F., Benzing, T., and Katsanis, N. (2011). Ciliopathies. N Engl J Med. 364, 1533-1543.

27. Braun, D.A., and Hildebrandt, F. (2017). Ciliopathies. Cold Spring Harb Perspect Biol. 9, a028191.
28. Reiter, J.F., and Leroux, M.R. (2017). Genes and molecular pathways underpinning ciliopathies. Nat Rev Mol Cell Biol. 18, 533-547.
29. Wheway, G., Mitchison, H.M., and Genomics England Research, C. (2019). Opportunities and Challenges for Molecular Understanding of Ciliopathies-The 100,000 Genomes Project. Front Genet. 10, 127.
30. Nachury, M.V. (2018). The molecular machines that traffic signaling receptors into and out of cilia. Curr Opin Cell Biol. 51, 124-131.
31. Jordan, M.A., and Pigino, G. (2021). The structural basis of intraflagellar transport at a glance. J Cell Sci. 134, jcs247163.
32. Walker, R.V., Keynton, J.L., Grimes, D.T., Sreekumar, V., Williams, D.J., Esapa, C., Wu, D., Knight, M.M., and Norris, D.P. (2019). Ciliary exclusion of Polycystin-2 promotes kidney cystogenesis in an autosomal dominant polycystic kidney disease model. Nat Commun. 10, 4072.
33. Garcia-Gonzalo, F.R., Corbit, K.C., Sirerol-Piquer, M.S., Ramaswami, G., Otto, E.A., Noriega, T.R., Seol, A.D., Robinson, J.F., Bennett, C.L., Josifova, D.J., et al. (2011). A transition zone complex regulates mammalian ciliogenesis and ciliary membrane composition. Nat Genet. 43, 776-784.
34. Legue, E., and Liem, K.F., Jr. (2019). Tulp3 Is a Ciliary Trafficking Gene that Regulates Polycystic Kidney Disease. Curr Biol. 29, 803-812 e805.
35. Ma, M., Tian, X., Igarashi, P., Pazour, G.J., and Somlo, S. (2013). Loss of cilia suppresses cyst growth in genetic models of autosomal dominant polycystic kidney disease. Nat Genet. 45, 1004-1012.
36. Schrier, R.W., Abebe, K.Z., Perrone, R.D., Torres, V.E., Braun, W.E., Steinman, T.I., Winklhofer, F.T., Brosnahan, G., Czarnecki, P.G., Hogan, M.C., et al. (2014). Blood pressure in early autosomal dominant polycystic kidney disease. N Engl J Med. 371, 2255-2266.
37. Torres, V.E., Abebe, K.Z., Chapman, A.B., Schrier, R.W., Braun, W.E., Steinman, T.I., Winklhofer, F.T., Brosnahan, G., Czarnecki, P.G., Hogan, M.C., et al. (2014). Angiotensin blockade in late autosomal dominant polycystic kidney disease. N Engl J Med. 371, 2267-2276.
38. Perrone, R.D., Abebe, K.Z., Watnick, T.J., Althouse, A.D., Hallows, K.R., Lalama, C.M., Miskulin, D.C., Seliger, S.L., Tao, C., Harris, P.C., et al. (2021). Primary results of the randomized trial of metformin administration in polycystic kidney disease (TAME PKD). Kidney Int. 100, 684-696.
39. Meijer, E., Visser, F.W., van Aerts, R.M.M., Blijdorp, C.J., Casteleijn, N.F., D'Agnolo, H.M.A., Dekker, S.E.I., Drenth, J.P.H., de Fijter, J.W., van Gastel, M.D.A., et al. (2018). Effect of Lanreotide on Kidney Function in Patients With Autosomal Dominant Polycystic Kidney Disease: The DIPAK 1 Randomized Clinical Trial. JAMA. 320, 2010-2019.
40. Grantham, J.J., Torres, V.E., Chapman, A.B., Guay-Woodford, L.M., Bae, K.T., King, B.F., Jr., Wetzel, L.H., Baumgarten, D.A., Kenney, P.J., Harris, P.C., et al. (2006). Volume progression in polycystic kidney disease. N Engl J Med. 354, 2122-2130.

41. Cornec-Le Gall, E., Audrezet, M.P., Rousseau, A., Hourmant, M., Renaudineau, E., Charasse, C., Morin, M.P., Moal, M.C., Dantal, J., Wehbe, B., et al. (2016). The PROPKD Score: A New Algorithm to Predict Renal Survival in Autosomal Dominant Polycystic Kidney Disease. J Am Soc Nephrol. 27, 942-951.
42. Messchendorp, A.L., Meijer, E., Visser, F.W., Engels, G.E., Kappert, P., Losekoot, M., Peters, D.J.M., and Gansevoort, R.T. (2019). Rapid Progression of Autosomal Dominant Polycystic Kidney Disease: Urinary Biomarkers as Predictors. Am J Nephrol. 50, 375-385.
43. Benson, K.A., Murray, S.L., Senum, S.R., Elhassan, E., Conlon, E.T., Kennedy, C., Conlon, S., Gilbert, E., Connaughton, D., O'Hara, P., et al. (2021). The genetic landscape of polycystic kidney disease in Ireland. Eur J Hum Genet. 29, 827-838.
44. Kline, T.L., Korfiatis, P., Edwards, M.E., Warner, J.D., Irazabal, M.V., King, B.F., Torres, V.E., and Erickson, B.J. (2016). Automatic total kidney volume measurement on follow-up magnetic resonance images to facilitate monitoring of autosomal dominant polycystic kidney disease progression. Nephrol Dial Transplant. 31, 241-248.
45. Levey, A.S., Stevens, L.A., Schmid, C.H., Zhang, Y.L., Castro, A.F., 3rd, Feldman, H.I., Kusek, J.W., Eggers, P., Van Lente, F., Greene, T., et al. (2009). A new equation to estimate glomerular filtration rate. Ann Intern Med. 150, 604-612.
46. Hopp, K., Cornec-Le Gall, E., Senum, S.R., Te Paske, I., Raj, S., Lavu, S., Baheti, S., Edwards, M.E., Madsen, C.D., Heyer, C.M., et al. (2020). Detection and characterization of mosaicism in autosomal dominant polycystic kidney disease. Kidney Int. 97, 370-382.
47. Richards, S., Aziz, N., Bale, S., Bick, D., Das, S., Gastier-Foster, J., Grody, W.W., Hegde, M., Lyon, E., Spector, E., et al. (2015). Standards and guidelines for the interpretation of sequence variants: a joint consensus recommendation of the American College of Medical Genetics and Genomics and the Association for Molecular Pathology. Genet Med. 17, 405-424.
48. Reese, M.G., Eeckman, F.H., Kulp, D., and Haussler, D. (1997). Improved splice site detection in Genie. J Comput Biol. 4, 311-323.
49. Desmet, F.O., Hamroun, D., Lalande, M., Collod-Beroud, G., Claustres, M., and Beroud, C. (2009). Human Splicing Finder: an online bioinformatics tool to predict splicing signals. Nucleic Acids Research. 37, e67.
50. Sudlow, C., Gallacher, J., Allen, N., Beral, V., Burton, P., Danesh, J., Downey, P., Elliott, P., Green, J., Landray, M., et al. (2015). UK biobank: an open access resource for identifying the causes of a wide range of complex diseases of middle and old age. PLoS Med. 12, e1001779.
51. Van Hout, C.V., Tachmazidou, I., Backman, J.D., Hoffman, J.D., Liu, D., Pandey, A.K., Gonzaga-Jauregui, C., Khalid, S., Ye, B., Banerjee, N., et al. (2020). Exome sequencing and characterization of 49,960 individuals in the UK Biobank. Nature. 586, 749-756.
52. Wang, Q., Dhindsa, R.S., Carss, K., Harper, A.R., Nag, A., Tachmazidou, I., Vitsios, D., Deevi, S.V.V., Mackay, A., Muthas, D., et al. (2021). Rare variant contribution to human disease in 281,104 UK Biobank exomes. Nature. 597, 527-532.
53. Pei, Y., Obaji, J., Dupuis, A., Paterson, A.D., Magistroni, R., Dicks, E., Parfrey, P., Cramer, B., Coto, E., Torra, R., et al. (2009). Unified criteria for ultrasonographic diagnosis of ADPKD. J Am Soc Nephrol. 20, 205-212.

54. Pei, Y., Hwang, Y.H., Conklin, J., Sundsbak, J.L., Heyer, C.M., Chan, W., Wang, K., He, N., Rattansingh, A., Atri, M., et al. (2015). Imaging-based diagnosis of autosomal dominant polycystic kidney disease. J Am Soc Nephrol. 26, 746-753.
55. Hirano, T., Katoh, Y., and Nakayama, K. (2017). Intraflagellar transport-A complex mediates ciliary entry and retrograde trafficking of ciliary G protein-coupled receptors. Mol Biol Cell. 28, 429-439.
56. Scheidel, N., and Blacque, O.E. (2018). Intraflagellar Transport Complex A Genes Differentially Regulate Cilium Formation and Transition Zone Gating. Curr Biol. 28, 3279-3287 e3272.
57. Picariello, T., Brown, J.M., Hou, Y., Swank, G., Cochran, D.A., King, O.D., Lechtreck, K., Pazour, G.J., and Witman, G.B. (2019). A global analysis of IFT-A function reveals specialization for transport of membrane-associated proteins into cilia. J Cell Sci. 132, jcs220749.
58. Perrault, I., Saunier, S., Hanein, S., Filhol, E., Bizet, A.A., Collins, F., Salih, M.A., Gerber, S., Delphin, N., Bigot, K., et al. (2012). Mainzer-Saldino syndrome is a ciliopathy caused by IFT140 mutations. Am J Hum Genet. 90, 864-870.
59. Schmidts, M., Frank, V., Eisenberger, T., Al Turki, S., Bizet, A.A., Antony, D., Rix, S., Decker, C., Bachmann, N., Bald, M., et al. (2013). Combined NGS approaches identify mutations in the intraflagellar transport gene IFT140 in skeletal ciliopathies with early progressive kidney Disease. Hum Mutat. 34, 714-724.
60. Bayat, A., Kerr, B., and Douzgou, S. (2017). The evolving craniofacial phenotype of a patient with Sensenbrenner syndrome caused by IFT140 compound heterozygous mutations. Clin Dysmorphol. 26, 247-251.
61. Hull, S., Owen, N., Islam, F., Tracey-White, D., Plagnol, V., Holder, G.E., Michaelides, M., Carss, K., Raymond, F.L., Rozet, J.M., et al. (2016). Nonsyndromic Retinal Dystrophy due to Bi-Allelic Mutations in the Ciliary Transport Gene IFT140. Invest Ophthalmol Vis Sci. 57, 1053-1062.
62. Xu, M., Yang, L., Wang, F., Li, H., Wang, X., Wang, W., Ge, Z., Wang, K., Zhao, L., Li, H., et al. (2015). Mutations in human IFT140 cause non-syndromic retinal degeneration. Hum Genet. 134, 1069-1078.
63. Jonassen, J.A., SanAgustin, J., Baker, S.P., and Pazour, G.J. (2012). Disruption of IFT complex A causes cystic kidneys without mitotic spindle misorientation. J Am Soc Nephrol. 23, 641-651.
64. Taliun, D., Harris, D.N., Kessler, M.D., Carlson, J., Szpiech, Z.A., Torres, R., Taliun, S.A.G., Corvelo, A., Gogarten, S.M., Kang, H.M., et al. (2021). Sequencing of 53,831 diverse genomes from the NHLBI TOPMed Program. Nature. 590, 290-299.
65. Pottel, H., Hoste, L., Dubourg, L., Ebert, N., Schaeffner, E., Eriksen, B.O., Melsom, T., Lamb, E.J., Rule, A.D., Turner, S.T., et al. (2016). An estimated glomerular filtration rate equation for the full age spectrum. Nephrol Dial Transplant. 31, 798-806.
66. Seliger, S.L., Watnick, T., Althouse, A.D., Perrone, R.D., Abebe, K.Z., Hallows, K.R., Miskulin, D.C., and Bae, K.T. (2020). Baseline Characteristics and Patient-Reported Outcomes of ADPKD Patients in the Multicenter TAME-PKD Clinical Trial. Kidney360. 1, 1363-1372.

67. Schrier, R.W., Johnson, A.M., McFann, K., and Chapman, A.B. (2003). The role of parental hypertension in the frequency and age of diagnosis of hypertension in offspring with autosomal-dominant polycystic kidney disease. Kidney Int. 64, 1792-1799.
68. Reed, B., McFann, K., Kimberling, W.J., Pei, Y., Gabow, P.A., Christopher, K., Petersen, E., Kelleher, C., Fain, P.R., Johnson, A., et al. (2008). Presence of de novo mutations in autosomal dominant polycystic kidney disease patients without family history. Am J Kidney Dis. 52, 1042-1050.
69. Waanders, E., te Morsche, R.H., de Man, R.A., Jansen, J.B., and Drenth, J.P. (2006). Extensive mutational analysis of PRKCSH and SEC63 broadens the spectrum of polycystic liver disease. Hum Mutat. 27, 830.
70. Besse, W., Choi, J., Ahram, D., Mane, S., Sanna-Cherchi, S., Torres, V., and Somlo, S. (2018). A noncoding variant in GANAB explains isolated polycystic liver disease (PCLD) in a large family. Hum Mutat. 39, 378-382.
71. Wilson, G.J., Wood, S., Patel, C., Oliver, K., John, G., Ranganathan, D., Mallett, A., and Isbel, N. (2020). DNAJB11-Related Atypical ADPKD in a Kidney Transplant Donor. Kidney Int Rep. 5, 1363-1366.
72. Delbarba, E., Econimo, L., Dordoni, C., Martin, E., Mazza, C., Savoldi, G., Alberici, F., Scolari, F., and Izzi, C. (2021). Expanding the variability of the ADPKD-GANAB clinical phenotype in a family of Italian ancestry. J Nephrol. Aug 6. doi: 10.1007/s40620-40021-01131-w. Online ahead of print.
73. Mallawaarachchi, A.C., Lundie, B., Hort, Y., Schonrock, N., Senum, S.R., Gayevskiy, V., Minoche, A.E., Hollway, G., Ohnesorg, T., Hinchcliffe, M., et al. (2021). Genomic diagnostics in polycystic kidney disease: an assessment of real-world use of whole-genome sequencing. Eur J Hum Genet. 29, 760-770.
74. Pei, Y., Paterson, A.D., Wang, K.R., He, N., Hefferton, D., Watnick, T., Germino, G.G., Parfrey, P., Somlo, S., and St. George-Hyslop, P. (2001). Bilineal disease and trans-heterozygotes in autosomal dominant polycystic kidney disease. Am J Hum Genet. 68, 355-363.
75. Bergmann, C., von Bothmer, J., Ortiz Bruchle, N., Venghaus, A., Frank, V., Fehrenbach, H., Hampel, T., Pape, L., Buske, A., Jonsson, J., et al. (2011). Mutations in multiple PKD genes may explain early and severe polycystic kidney disease. J Am Soc Nephrol. 22, 2047-2056.
76. Fedeles, S.V., Tian, X., Gallagher, A.R., Mitobe, M., Nishio, S., Lee, S.H., Cai, Y., Geng, L., Crews, C.M., and Somlo, S. (2011). A genetic interaction network of five genes for human polycystic kidney and liver diseases defines polycystin-1 as the central determinant of cyst formation. Nat Genet. 43, 639-647.
77. Gainullin, V.G., Hopp, K., Ward, C.J., Hommerding, C.J., and Harris, P.C. (2015). Polycystin-1 maturation requires polycystin-2 in a dose-dependent manner. J Clin Invest. 125, 607-620.
78. Olson, R.J., Hopp, K., Wells, H., Smith, J.M., Furtado, J., Constans, M.M., Escobar, D.L., Geurts, A.M., Torres, V.E., and Harris, P.C. (2019). Synergistic Genetic Interactions between Pkhd1 and Pkd1 Result in an ARPKD-Like Phenotype in Murine Models. J Am Soc Nephrol. 30, 2113-2127.

79. Vujic, M., Heyer, C.M., Ars, E., Hopp, K., Markoff, A., Orndal, C., Rudenhed, B., Nasr, S.H., Torres, V.E., Torra, R., et al. (2010). Incompletely penetrant *PKD1* alleles mimic the renal manifestations of ARPKD. J Am Soc Nephrol. 21, 1097-1102.
80. Audrezet, M.P., Corbiere, C., Lebbah, S., Moriniere, V., Broux, F., Louillet, F., Fischbach, M., Zaloszyc, A., Cloarec, S., Merieau, E., et al. (2016). Comprehensive PKD1 and PKD2 Mutation Analysis in Prenatal Autosomal Dominant Polycystic Kidney Disease. J Am Soc Nephrol. 27, 722-729.
81. Losekoot, M., Ruivenkamp, C.A., Tholens, A.P., Grimbergen, J.E., Vijfhuizen, L., Vermeer, S., Dijkman, H.B., Cornelissen, E.A., Bongers, E.M., and Peters, D.J. (2012). Neonatal onset autosomal dominant polycystic kidney disease (ADPKD) in a patient homozygous for a PKD2 missense mutation due to uniparental disomy. J Med Genet. 49, 37-40.
82. Jordan, P., Arrondel, C., Bessieres, B., Tessier, A., Attie-Bitach, T., Guterman, S., Moriniere, V., Antignac, C., Saunier, S., Gubler, M.C., et al. (2021). Bi-allelic pathogenic variations in DNAJB11 cause Ivemark II syndrome, a renal-hepatic-pancreatic dysplasia. Kidney Int. 99, 405-409.
83. Ateş, E.A., Turkyilmaz, A., Delil, K., Alavanda, C., Söylemez, M.A., Geçkinli, B.B., Ata, P., and Arman, A. (2021). Biallelic Mutations in DNAJB11 are Associated with Prenatal Polycystic Kidney Disease in a Turkish Family. Mol Syndromol. 12, 179-185.
84. Frank, C.G., Grubenmann, C.E., Eyaid, W., Berger, E.G., Aebi, M., and Hennet, T. (2004). Identification and functional analysis of a defect in the human ALG9 gene: definition of congenital disorder of glycosylation type IL. Am J Hum Genet. 75, 146-150.
85. Chantret, I., Dancourt, J., Dupré, T., Delenda, C., Bucher, S., Vuillaumier-Barrot, S., Ogier de Baulny, H., Peletan, C., Danos, O., Seta, N., et al. (2003). A deficiency in dolichyl-P-glucose:Glc1Man9GlcNAc2-PP-dolichyl alpha3-glucosyltransferase defines a new subtype of congenital disorders of glycosylation. J Biol Chem. 278, 9962-9971.
86. Lu, W., Peissel, B., Babakhanlou, H., Pavlova, A., Geng, L., Fan, X., Larson, C., Brent, G., and Zhou, J. (1997). Perinatal lethality with kidney and pancreas defects in mice with a targeted *Pkd1* mutation. Nature Genet. 17, 179-181.
87. Bergmann, C., Senderek, J., Sedlacek, B., Pegiazoglou, I., Puglia, P., Eggermann, T., Rudnik-Schoneborn, S., Furu, L., Onuchic, L.F., De Baca, M., et al. (2003). Spectrum of mutations in the gene for autosomal recessive polycystic kidney disease (ARPKD/PKHD1). J Am Soc Nephrol. 14, 76-89.
88. Hopp, K., Ward, C.J., Hommerding, C.J., Nasr, S.H., Tuan, H.F., Gainullin, V.G., Rossetti, S., Torres, V.E., and Harris, P.C. (2012). Functional polycystin-1 dosage governs autosomal dominant polycystic kidney disease severity. J Clin Invest. 122, 4257-4273.
89. Qian, F., Watnick, T.J., Onuchic, L.F., and Germino, G.G. (1996). The molecular basis of focal cyst formation in human autosomal dominant polycystic kidney disease type I. Cell. 87, 979-987.
90. Piontek, K., Menezes, L.F., Garcia-Gonzalez, M.A., Huso, D.L., and Germino, G.G. (2007). A critical developmental switch defines the kinetics of kidney cyst formation after loss of Pkd1. Nat Med. 13, 1490-1495.
91. Tan, A.Y., Zhang, T., Michaeel, A., Blumenfeld, J., Liu, G., Zhang, W., Zhang, Z., Zhu, Y., Rennert, L., Martin, C., et al. (2018). Somatic Mutations in Renal Cyst Epithelium in Autosomal Dominant Polycystic Kidney Disease. J Am Soc Nephrol. 29, 2139-2156.

92. Lantinga-van Leeuwen, I.S., Dauwerse, J.G., Baelde, H.J., Leonhard, W.N., van de Wal, A., Ward, C.J., Verbeek, S., DeRuiter, M.C., Breuning, M.H., de Heer, E., et al. (2004). Lowering of Pkd1 expression is sufficient to cause polycystic kidney disease. Hum Mol Genet. 13, 3069-3077.
93. Rossetti, S., Kubly, V.J., Consugar, M.B., Hopp, K., Roy, S., Horsley, S.W., Chauveau, D., Rees, L., Barratt, T.M., van't Hoff, W.G., et al. (2009). Incompletely penetrant PKD1 alleles suggest a role for gene dosage in cyst initiation in polycystic kidney disease. Kidney Int. 75, 848-855.
94. Durkie, M., Chong, J., Valluru, M.K., Harris, P.C., and Ong, A.C.M. (2021). Biallelic inheritance of hypomorphic PKD1 variants is highly prevalent in very early onset polycystic kidney disease. Genet Med. 23, 689-697.
95. Brasier, J.L., and Henske, E.P. (1997). Loss of the polycystic kidney disease (*PKD1*) region of chromosome 16p13 in renal cyst cells supports a loss-of-function model for cyst pathogenesis. J Clin Invest. 99, 194-199.
96. Brook-Carter, P.T., Peral, B., Ward, C.J., Thompson, P., Hughes, J., Maheshwar, M.M., Nellist, M., Gamble, V., Harris, P.C., and Sampson, J.R. (1994). Deletion of the *TSC2* and *PKD1* genes associated with severe infantile polycystic kidney disease – a contiguous gene syndrome. Nat Genet. 8, 328-332.
97. Sampson, J.R., Maheshwar, M.M., Aspinwall, R., Thompson, P., Cheadle, J.P., Ravine, D., Roy, S., Haan, E., Bernstein, J., and Harris, P.C. (1997). Renal cystic disease in tuberous sclerosis: role of the polycystic kidney disease 1 gene. Am J Hum Genet. 61, 843-851.

FIGURE LEGENDS

Figure 1: Details of the study design: (**A**) The study is divided into screening of ADPKD spectrum families (Part 1) and analysis of previously sequenced cohorts (Part 2). Part 1 included subjects from ADPKD clinical trials: HALT PKD (HALT), DIPAK randomized clinical trial (RCT), and TAME; ADPKD observational studies: CRISP, DIPAC Observational (Observ), and Genkyst; genetics studies, ADPKD Modifier, Mayo PKD Center, and Irish Kidney Gene Project (IKGP), and other recruitment sites, Sheffield, Tufts, Brest, and Kuwait, while Part 2 consisted of the Genomics England 100K project Cystic Kidney Disease cohort (100kG; PKD) and the UK Biobank (individuals with ICD-10 Q61). The number of analyzed individuals per study site is indicated. (**B**) The sequencing methods and whether participants were prescreened for *PKD1* and *PKD2* are indicated, with the total number of screened and IFT140 positive families shown. The number of families/probands with pathogenic *IFT140* variants relative to the total number screened by each method from each study/site are shown above. Out of the 777 naïve families screened at Mayo, 357 (45.9%) and 105 (13.5%) were resolved by pathogenic or likely pathogenic *PKD1* or *PKD2* variants, respectively, while 30 (3.9%) and 6 (0.8%) had a VUS to *PKD1* or *PKD2.* Amongst the pathogenic variants were 19 *PKD1* large deletions, 1 *PKD1* large duplication, and 3 *PKD2* large deletions. The relatively low number of families resolved with a *PKD1* or *PKD2* pathogenic variant (59.5%), reflects the broad phenotypic spectrum of the recruited individuals, including mild cystogenesis. (**C**) Summary of the screening showing the total number of IFT140 families identified by screening of ADPKD spectrum subjects (Part 1) and identified in the 100kG, PKD cohort and the UK Biobank (Part 2).

Figure 2: Pedigree and imaging details of 5 IFT140 pedigrees. Pedigrees M132 (**A**), M199 (**G**), P1320 (**L**), EDI1005 (**O**), and 390044 (**S**) with clinically affected individuals in black, unaffected in white, and uncertain in gray, with deceased subjects lined through. Only affected individuals or others with a sample available are shown. (**A**) In M132 segregation of the *IFT140* pathogenic variant and *PKD1* VUS are shown; *IFT140:* c.2399+1G>T and *PKD1*: c.11017-3C>T cosegregate. (**G**) In M199 inheritance of *IFT140*: c.2767_27688+2del and a frameshifting variant in *DYNC2H1* (biallelically causing SRTD3), that does not segregate with the disease, are shown. In P1320 (**L**), the *IFT140* pathogenic variant segregates in 4 individuals with a *PKD1* VUS, while a *BBS2* VUS does not cosegregate with disease. EDI1005 (**O**) just had an *IFT140* pathogenic variant. Two *PKD1* VUS cosegregated with the *IFT140* pathogenic variant in 390044 (**S**). It is not known if these additional variants have any influence on the disease phenotype (see Table 3 for details). Abdominal coronal imaging by MRI (**B**-**D**, **J, M, N, Q**) or CT (**E**, **F, P, T, V**), axial imaging by CT (**H, I, K, U**), or abdominal ultrasound (US) (**R**) with the age at imaging indicated shows the kidney phenotype is typically multiple, larger bilateral cysts, sometimes with marked asymmetry (**K**). Only M132 IV-1 (**F**) has liver cysts.

Figure 3: Pedigrees and imaging details of 7 IFT140 families. Pedigrees of M1629 (**A**), PK14083 (**D**), M1554 (**G**), P1497 (**J**), 1470059 (**M**), M1169 (**P**), and M1266 (**R**), with clinically affected individuals in black, unaffected in white, and uncertain in gray, with deceased subjects lined through. Only affected individuals or others with a sample available are shown. The segregation of the *IFT140* pathogenic variant in each family is shown (inferred in M1629 III-1), plus inheritance of variants in *PKD1*; *in cis* with the *IFT140* pathogenic variant in M1629 and 1470059. Variants of uncertain significance to *PKHD1* (M1554 and M1266), that cosegregate with disease, and *WDR35* (M1554) that does not, are also noted. It is not known if these additional variants have any influence on the disease phenotype (see Table 3 for details). Abdominal coronal MRI (**C**, **E, F**, **K**, **L**, **N, O, S**), coronal (**B**, **H**, **Q**) or axial CT (**I**) with the age at imaging indicated shows the kidney and liver phenotypes. The cystic presentation varies from several large cysts bilaterally (**N**), to much milder cystogenesis (**O, S**).

Figure 4. UK biobank data demonstrates *IFT140* LoF alleles are associated with cystic kidney disease: (A) Gene-level Manhattan association plot with binary trait Q61 (Cystic Kidney Disease) and Fisher's exact two-sided test statistics. A significance threshold of $P \leq 2 \times 10^{-9}$ has been selected (see Methods). Here, gene-level results are shown using a collapsing model based on protein truncating variants with a gnomAD MAF of ≤5% (ptv5pcnt). The proportion of cases with a qualifying protein truncating variants in the Q61 group (n=521) was compared with the proportion in controls (n=239,516) for each gene. Among the 521 cases, 14 (2.69%) had a monoallelic *IFT140* truncating variant, compared to 506 (0.21%) among the controls. For *PKD1*, *PKD2* and *ALG9*; 44 (8.45%) cases and 35 (0.015%) controls; 29 (5.57%) cases and 10 (0.004%) controls; and 4 (0.77%) cases and 76 (0.032%) controls had a monoallelic truncating variant, respectively. The -log10 p-values for enrichment in the Cystic Kidney Disease group are shown, with *ALG9* not reaching the significance threshold. Graph generated from the Astra Zeneca PheWAS Portal[52] (**B**) Prevalence of kidney-related diagnoses in *IFT140* High (likely pathogenic) vs. Low Impact (likely benign) variant carriers. Of the 200,643 individuals from the UK Biobank with exome data, 481 had monoallelic High and 5,888 Low Impact variants to *IFT140*. Comparison of individuals with kidney-related diagnoses (grouped by ICD-10 terms) showed that Cyst of Kidney (N28.1), Cystic Kidney Disease (Q61) and CKD stages 4 & 5 (N18.4 & N18.5) were significantly more common in individuals with High Impact *IFT140* variants compared to Low Impact (shaded; see figure for p=values and odds ratios with 95% Confidence Intervals; CI). One High Impact carrier was in both the N28.1 and Q61 groups. Other kidney phenotypes were not enriched for High Impact *IFT140* variants.

Figure 5: Comparison of eGFR and htTKV between IFT140 and PKD2 individuals. (A) Plotting of eGFR values versus age demonstrates that IFT140 individuals have a slower decline in renal function compared to PKD2[8; 9], but quicker than would be expected with normal aging. Only 1 IFT140 subject reached ESKD, and 1 had CKD stage 4. (B) Plot of height adjusted TKV on the natural log scale (In htTKV) versus age for individuals with a typical and atypical MIC differentiated compared to PKD2[8; 9]. A wide range of htTKV are seen associated with ADPKD-*IFT140*. Shading shows the 95% confidence intervals.

Table 1: Details of individuals with *IFT140* pathogenic variants

Demographics				Clinical Details				Kidney Imaging						
Pedigree[b] (Study)	Subject[c]	Sex	Dx age[a]	eGFR[a], age	HTN, age	Type	Age	Cyst Description[f]	Volume (mL/m) or length (c)[g] htRK	htLK	htTKV	MIC	Fig	Liver Cysts [a,h]
Families														
M132	I-2[d]	F	NA	NA	Y, ?	NA	-	MLg RKN	-	-	-	-	-	NA
(Mayo)	II-1[d]	M	NA	43, 94y	Y, ?	CT	91y	BMLg LKEx	221	427	648	2A	2E	NA
	II-2[e]	M	NA	46, 72y	Y, ?	NA	-	BLg	-	-	-	-	-	NA
	II-3	M	69y	66, 74y	N, ?	MRI	69y	BMLg LKEx	360	566	926	1B	2B	N
	III-1	M	54y	47, 66y	N, ?	MRI	63y	BM	393	436	830	1B	2C	N
	III-2	M	40y	109, 47y	N, ?	MRI	45y	BCl	425	197	622	2A	2D	N
	IV-1[d]	F	38y	81, 38y	N, 39y	CT	38y	RKFLg LKDP	89	79	169	2A	2F	2S
M199	II-1	F	59y	57, 87y	Y, <72y	CT	81y	BFEx	-	-	-	2A	2H	NA
(Mayo)	II-2 [d]	M	NA	21, 70y	NA	NA	-	-	-	-	-	-	-	NA
	II-3 [d]	M	77y	41, 78y	Y, <75y	CT	77y	BMEx	308	454	762	1B	2I	N
	II-4	M	74y	35, 74y	Y, <42y	US	74y	BLg	-	-	-	-	S1A,B	N
	III-1	F	39y	55, 73y	N, 74y	MRI	57y	BLgEx	166	106	272	2A	2J	N
	III-2	F	58y	87, 71y	Y, 63y	CT	58y	BF LK1Lg	10.9c	13.6c	-	2A	2K	N
	III-4	M	-	38, 72y	Y, <68y	CT	69y	BFCl	170	131	301	2A	S1C	N
P1320	II-1	F	69y	46, 77y	Y, ?	MRI	69y	BMLg	17.9c	15.4c	-	-	2M	1
(Shef)	II-2	F	66y	73, 69y	Y, ?	US	66y	BFLg	13c	13c	-	-	-	N
	III-2	F	46y	58, 52y	NA	MRI	46y	LK1 RK5	10.7c	13.2c	-	2A	2N	N
	III-4	M	40y	94, 43y	NA	US	40y	BMLg	12.4c	12.9c	-	-	-	N
EDI1005	I-1[d]	M	80y	NA	NA	Autopsy	89y	BLg	-	-	-	-	-	NA
(100kG)	II-1	F	NA	56, 68y	Y, ?	CT	58y	BMLg	1340	966	2306	1D	2P	FS
	III-1	M	33y	99, 37y	N, 37y	MRI	33y	BMLg	540	262	802	1D	2Q	N
	III-2	F	30y	85, 39y	N, 39y	US	37y	BMLg	-	-	-	-	2R	N
390044	II-1[d]	F	-	59, 86y	Y, 66y	CT	86y	MLg RKN	N	253	-	-	2V	N
(HALT)	II-2	F	63y	51, 79y	Y, <65y	CT	63y	FLg LKN	-	-	-	-	2U	F
	III-1	F	41y	45, 58y	Y, 37y	CT	58y	BMEx	348	864	1212	1C	2T	N
M1629	II-1	M	71y	39, 73y	Y,<61y	MRI	71y	BMLg&S	450	517	967	1B	3C	FS
(Mayo)	III-1	M	40y	80, 40y	Y, <40y	US	40y	BFLg	11.1c	11.2c	-	-	S1D	N
	III-2	F	39y	107, 40y	N, 40y	CT	39y	BF	137	134	272	1B	3B	FS
PK14083	II-1	M	62y	57,65y	Y, 55y	MRI	62y	BLgEx	333	508	841	2A	3E	N
(Brest)	II-2	F	58y	37, 63y	Y, 55y	MRI	62y	MBLg	177	221	398	2A	3F	N
M1554	II-1	F	53y	82, 57y	Y, <53y	CT	53y	A LKFLg	10.5c	18.8c	-	2A	3H	N
(Tufts)	III-1	F	34y	84, 36y	N, 36y	CT	34y	U RKMLg	-	-	-	2A	3I	N
P1497	II-1	F	51y	85, 56y	Y, 51y	MRI	57y	A LKMLg	773	329	1102	2A	3K	N
(DIPAK^R)	II-2	F	39y	83, 54y	N, 54y	MRI	54y	A LKM RKFS	114	219	333	2A	3L	N
1470059	II-1	M	72y	44, 79y	Y, 54y	MRI	76y	BMLgEx	822	952	1774	1C	3N	N
(Mod)	III-1	M	45y	84, 49y	N, 49y	MRI	49y	BFSEx	114	159	273	1A	3O	N
M1169	I-1	M	-	50, 84y	Y, 81y	US	?	2 LK	-	-	-	-	-	NA
(Mayo)	II-1	F	46y	102, 50y	N, 50y	CT	46y	BF	141	163	304	1B	3Q	N

Pedigree[b] (Study)	Subject[c]	Sex	Dx age[a]	eGFR[a], age	HTN age	Type	Age	Cyst Description[f]	Volume (mL/m) or length (c)[g] htRK	htLK	htTKV	MIC	Fig	Liver Cysts [a, h]
M1266 (Mayo)	II-1	F	-	65, 67y	N, 67y	US	66y	BM FLg	9.6c	9.3c	-	-	-	N
	II-2	F	45y	80, 58y	N, 59y	MRI	55y	FS	67	69	136	1A	3S	MnS
Singletons														
440003 (CRISP)	406737	F	41y	74, 54y	N, 54y	MRI	53y	BF	199	107	307	1A	S2A	N
690036 (HALT)	E4669644	M	51y	38, 68y	Y, 51y	US	58y	BM	-	-	-	-	-	-
F430 (Dublin)	8143	M	31y	67, 45y	N, 46y	US	31y	BF	12.6c	12c	-	-	-	N
F392 (Dublin)	10235	F	45y	94, 58y	Y, 50y	US	45y	BMLg	9.7c	10.7c	-	2A	S1E	N
F662 (Dublin)	10664	F	NA	69, 76y	Y, 58y	US	70y	A RK2Lg LKMLg	14.8c	11.2c	-	-	S1F	N
M120 (Mayo)	R1097	F	46y	70, 65y	Y, 45y	MRI	65y	BMEx RK1Lg	296	222	519	2A	S3F	N
M154 (Mayo)	R1142	F	57y	68, 64y	Y, <50y	CT	64y	A BMLg	451	946	1397	2A	S2B	N
M187 (Mayo)	R19	F	53y	35, 79y	Y, 53y	CT	78y	BMLg	1025	994	2019	1C	S2C	N
M241 (Mayo)	R1403	M	74y	30, 85y	Y, <69y	CT	83y	BMLg	498	562	1060	1A	S2D	N
M274 (Mayo)	R1367	F	72y	43, 90y	Y, <72y	MRI	79y	A LKFLg RKS	81	375	455	2A	S2E	N
M323 (Mayo)	R1606	M	58y	41, 67y	Y, <68y	US	67y	BMLg	-	-	-	-	-	N
M357 (Mayo)	R874	F	50y	49, 76y	Y, <62y	CT	76y	A LKFL RKM	1325	471	1796	2A	S2F	N
M614 (Mayo)	R1942	M	46y	82, 59y	Y, 45y	CT	53y	BFLgEx	353	253	606	2A	S2G	N
M1062 (Mayo)	R2939	M	56y	52, 62y	Y, 55y	CT	62y	A RK<5Lg LK 1Lg	776	359	1135	2A	S2H	N
M1111 (Mayo)	R2995	M	50y	46, 55y	N, 52y	MRI	52y	BFS	101	122	222	1A	S2I	N
M1261 (Tufts)	R3221	F	29y	99, 34y	N, 32y	CT	30y	FS RK1Lg	217	158	375	2A	S2J	N
M1277 (Mayo)	R3248	M	56y	ESKD, 64y	Y, 56y	CT	61y	RKN WT6m LKMEx	N	261	-	-	S3A	FS
M1374 (Mayo)	R3376	F	65y	62, 68y	Y, 67y	CT	68y	BFLK1Lg	927	562	1489	2A	S2K	N
M1540 (Mayo)	R2098	M	64y	57, 65y	Y, <65y	CT	66y	BFEx	152	315	468	1B	S3D	N
P1195 (Shef)	Ox3922	F	57y	50, 92y	Y, ?	CT	92y	BMLgEx	17c	23c	-	-	S2L	N
P1480 (Kuw)	Ox5181	F	44y	130, 44y	Y, 40y	US	44y	LK8 RK8	456	420	876	1C	-	N
P1504 (DIPAK^{O})	Ox5058	M	52y	43, 57y	Y, 48y	MRI	61y	MBLg	1371	1376	2747	1D	S2M	M
P1505 (TAME)	Ox5262	F	50y	70, 52y	Y, 41y	MRI	52y	A LK2Lg RK FS	179	709	888	2A	S2N	N
PK14084 (Genkyst)	210192	F	37y	105, 48y	N, 48y	MRI	48y	FBLg	218	158	376	2A	S3H	N
PK14082 (Brest)	200138	F	44y	77, 44y	N, 44y	CT	44y	FBLg	109	170	270	2A	S2O	N
PK14085 (Brest)	210193	F	75y	57,75y	N, 75y	CT	75y	FBLg	142	106	248	2A	S2P	N

[a] NA, not available. [b]DIPAK^{R}, DIPAK randomized clinical trial; 100kG, 100,000 Genomes; Kuw, Kuwait; Mod, Modifiers of PKD Study; Shef, Sheffield; DIPAK^{O}, DIPAK Observational Study; [c] [d]no sample for genetic confirmation; [e]genotype inferred; [f]A, asymmetric presentation; B, bilateral; Cl, clustered, DP, dilated pelvis; Ex, some exophytic; F, few, LK, left kidney; Lg large; M, multiple; Mn, many; N, nephrectomy; RK, right kidney, S, small; U, unilateral; WT, Wilms tumor. [g]htRK, height adjusted right kidney volume; htLK, height adjusted left kidney volume; htTKV, height adjusted left kidney volume; [h]F, few; Mn, many; N, none; S, small.

Table 2: Details of the *IFT140* pathogenic variants

cDNA variant[a]	Protein variant	Type[b]	Effect[c]	GnomAD v2.1.1	Publication	ClinVar	ACMG Designation[d]	Part 1 Pedigrees	100,000 Genomes Pedigrees
c.223delG	p.Val75fs*11	FS del	Truncating	0	-	N	LP	M1266	-
c.490G>T	p.Glu164*	Nonsense	Truncating	0	[59]	N	P	F392, M614, M1261	-
c.581delT	p.Leu194fs*2	FS del	Truncating	0	-	N	LP	440003	-
c.594dupG	p.Ser199fs*21	FS dup	Truncating	0	-	N	LP	M1374	-
c.634G>A	p.Gly212?	Splice	Non Trunc	15/282764	[58]	8x P, 2x LP	LP	M1277	-
c.810+1G>A	p.Lys270?	Splice	Truncating	0	-	N	LP	-	UK25
c.931dupT	p.Tyr311fs*7	FS dup	Truncating	0	-	N	LP	690036	-
c.992_993del	p.Cys331fs*3	FS del	Truncating	0	-	N	LP	EDI1005	-
c.1010-1G>A	p.Gly337?	Splice	Truncating	11/279352	-	5x P	P	F662, PK14082	-
c.1039C>T	p.Arg347*	Nonsense	Truncating	1/250764	-	N	LP	-	UK11
c.1147C>T	p.Gln383*	Nonsense	Truncating	1/31360	-	N	LP	-	UK4
c.1246C>T	p.Gln416*	Nonsense	Truncating	6/249758	-	N	LP	-	UK10, UK17
c.1359+1G>A	p.Lys453?	Splice	Truncating	0	-	1x LP	LP	-	UK16
c.1377G>A	p.Trp459*	Nonsense	Truncating	22/215228	[62]	1x P	P	M241, M274, M1169, P1505	UK12, UK14, UK26
c.1525-1G>A	p.Gly509?	Splice	Truncating	0	-	1x LP	LP	P1480	-
c.1565G>A	p.Gly522Glu	Missense	Non Trunc	39/282790	[58]	5x P, 1x VUS	LP	M1540	-
c.1648C>T	p.Arg550*	Nonsense	Truncating	0	-	N	P	PK14085	UK9
c.1653-1G>A	p.Arg551?	Splice	Truncating	0	-	N	P	M1111	-
c.1655_1656del	p.Glu552fs*6	FS del	Truncating	0	[62]	N	P	P1497, 1470059	-
c.1959G>A	p.Trp653*	Nonsense	Truncating	4/280738	-	1x P, 1x VUS	LP	-	UK13
c.2278C>T	p.Arg760*	Nonsense	Truncating	0	[59]	1x P	P	F430	UK1
c.2285_2286del	p.Phe762fs*39	FS del	Truncating	0	-	N	LP	P1320	-
c.2399+1G>T	p.Ser800?	Splice	Truncating	14/251478	[58]	5x P	P	M132, M154, M187, M323, M357, P1195, P1504	UK2, UK3, UK6, UK7, UK15, UK18, UK19, UK21, UK22, UK23, UK24, UK27
c.2400-2A>T	p.Ser800?	Splice	Truncating	0	-	1x P	LP	M1629	-
c.2483delG	p.Gly828fs*18	FS del	Truncating	0	-	N	LP	390044	-
c.2500C>T	p.Arg834*	Nonsense	Truncating	2/256536	-	1x P	LP	-	UK8
c.2542_2559del	p.Arg848_Ala853del	IF del	Non Trunc	0	-	N	LP	PK14084	-
c.2767_2768+2del	p.Tyr923fs*18	Splice	Truncating	8/148,386	-	2x LP	LP	M199, M1062, M1554	-
c.2909_2920del	p.Glu970_Ala973del	IF del	Non Trunc	2/281,118	-	N	LP	M120	-
c.2998-1G>A	p.Lys999?	Splice	Truncating	0	-	N	LP	-	UK20
c.3214C>T	p.Arg1072*	Nonsense	Truncating	3/249956	-	N	LP	-	UK5
c.3696del	p.Ile1234Serfs*33	FS del	Truncating	0	-	N	LP	PK14083	

[a] RefSeq transcript # NM_014714.4; [b] FS del, frameshift deletion; FS dup, frameshift duplication; IF del, inframe deletion; [c] Non Trunc, nontruncating; [d] P, pathogenic; LP, likely pathogenic, VUS, variant of uncertain significance.

Table 3: Details of other variants of interest

IFT140 pathogenic variant	Gene	cDNA variant [a]	Protein variant	Type[b]	Effect[c]	CADD Score [d]	ACMG Des[e]	PKD DB [f]	GnomAD v2.1.1	ClinVar[e]	Individuals	Pedigree
c.223delG (Val75fs*11)	*PKHD1*	c.3549delT	p.His1184fs*36	FS del	Trunc	NA	LP[R]	-	0	1x P	II-1, II-2	M1266
c.490G>T (p.Glu164*)	*TMEM231*	c.248C>A	p.Ser83*	Nons	Trunc	NA	LP[R]	-	0	N	10235	F392
c.581delT (p.Leu194fs*2)	*COL4A1*	c.1612C>T	p.Arg538Trp	Mis	Non Trunc	23.9	VUS	-	4/251364	N	406737	440003
	PKD1	c.2032G>T	p.Ala678Ser	Mis	Non Trunc	4.00	VUS	No	0	N		
	PKD1	c.4055G>A	p.Ser1352Asn	Mis	Non Trunc	14.34	VUS	VUS	186/279278	1x LB, 2x VUS		
c.594dupG (p.Ser199fs*21)	*PKD1*	c.4055G>A	p.Ser1352Asn	Mis	Non Trunc	14.34	VUS	VUS	186/279278	1x LB, 2x VUS	R3376	M1374
c.634G>A (p.Gly212?)	*PKD1*	c.8293C>T	p.Arg2765Cys	Mis	Non Trunc	29.20	VUS	M	1299/278546	1x B, 2x VUS, 2x LP	R3248	M1277
c.1010-1G>A (p.Gly337?)	*PKD1*	c.4963G>A	p.Val1655Met	Mis	Non Trunc	0.05	LB	No	15/279582	N	10664	F662
	TTC21B	c.2318C>A	p.Ser773*	Nons	Trunc	NA	LP[R]	-	0	N		
c.3214C>T (p.Arg1072*)	*PKD1*	c.3019G>A	p.Val1007Met	Mis	Non Trunc	22.70	VUS	No	5/244386	1xVUS	*UK5-1*	*UK5*
c.1377G>A (p.Trp459*)	*WDR60*	c.69G>A	p.Trp23*	Nons	Trunc	NA	VUS	-	84/248930	1x P, 2x VUS	R1403	M241
	ALG9	c.551T>G	p.Phe184Cys	Mis	Non Trunc		VUS	-	18/280924	N	R1367	M274
	PKD2	c.112G>C	p.Ala38Pro	Mis	Non Trunc	18.48	VUS	No	0	N		
	OFD1	c.936-2A>G	p.Asn313?	Splice	Trunc	NA	VUS	-	24/202878	1x B, 2x VUS	Ox5262	P1505
c.1565G>A (p.Gly522Glu)	*PKHD1*	c.1018G>A	p.Gly340Arg	Mis	Non Trunc	16.58	VUS	-	16/282680	2x VUS	R2098	M1540
c.1653-1G>A, p.Arg551?	*CEP290*	c.1066G>A	p.Gly356Ser	Mis	Non Trunc	31.0	VUS	-	0	N	R2995	M1111
c.1655_1656del (p.Glu552fs*6)	*PKD1*	c.4073C>T	p.Ala1358Val	Mis	Non Trunc	6.77	LB	No	17/279412	N	II-1, III-1	1470059
c.1963C>T (p.Gln655*)	*PKD1*	c.4265C>A	p.Ala1422Asp	Mis	Non Trunc	3.77	VUS	No	2/249058	N	Ox5310, Ox5538	P1506?
c.2278C>T (p.Arg760*)	*PKD1*	c.113T>A	p.Leu38His	Mis	Non Trunc	22.60	VUS	No	0	N	8143	F430
	TMEM260	c.721dupT	p.Tyr241fs*3	FS dup	Trunc	NA	LP[R]	-	6/251474	1x P		
c.2285_2286del (p.Phe762fs*39)	*PKD1*	c.3077C>T	p.Thr1026Ile	Mis	Non Trunc	18.23	LB	LN	12/278272	N	all II2, II3	P1320
	BBS2	c.823C>T	p.Arg275*	Nons	Trunc	NA	LP	-	54/282748	12x P		
c.2399+1G>T (p.Ser800?)	*PKD1*	c.11017-3C>T	p.Arg3672?	Splice	Non Trunc	NA	LB	LN	298/279962	3x VUS	II-2, II-3, III-1, III-2 R1142, R19	M132, M154, M187
	PKD1	c.10601C>T	p.Ala3534Val	Mis	Non Trunc	18.22	LB	No	43/238314	N	III-2	M132
	DZIP1L	c.544C>T	p.Arg182Trp	Mis	Non Trunc	31.0	VUS	-	6/278088	N	R1142	M154
	PKD1	c.8293C>T	p.Arg2765Cys	Mis	Non Trunc	29.20	VUS	M	1299/278546	1x B, 2x VUS, 2x LP	R1606	M323
	IFT43	c.343C>T	p.Gln115*	Nons	Trunc	NA	LP[R]	-	12/282886	N	Ox5058	P1504
	PKD1	c.360-5T>G	p.Ile120?	Splice	Non Trunc	NA	VUS	No	0	N	*UK27-1*	*UK27*

IFT140 pathogenic variant	Gene	cDNA variant [a]	Protein variant	Type[b]	Effect[c]	CADD Score [d]	ACMG Des[e]	PKD DB [f]	GnomAD v2.1.1	ClinVar[e]	Individuals	Pedigree
c.2400-2A>T (p.Ser800?)	*PKD1*	c.2990C>T	p.Thr997Met	Mis	Non Trunc	23.60	VUS	No	2/240882	N	II-1, III-2	M1629
c.2483delG (p.Gly828fs*18)	*PKD1*	c.8293C>T	p.Arg2765Cys	Mis	Non Trunc	29.20	VUS	M	1299/278546	1x B, 2x VUS, 2x LP	II-2	390044
	PKD1	c.7636C>T	p.His2546Tyr	Mis	Non Trunc	17.69	VUS	LN	411/251160	2x B, 1x LB, 1x VUS	II-2, III-2	390044
c.2767_2768+2del (p.Tyr923fs*18)	*DYNC2H1*	c.3054delT	p.Phe1018fs*3	FS del	Trunc	NA	LP[R]	-	0	N	III-2	M199
	PKD1	c.2098-3C>T	p.Val700?	Splice	Non Trunc	NA	LB	No	7/133582	LB	R2939	M1062
	PKHD1	c.1822G>T	p.Asp608Tyr	Mis	Non Trunc	21.8	VUS	-	1/246468	N	II-1, III-1, II-1	M1554
	WDR35	c.205G>A	p.Gly69Ser	Mis	Non Trunc	28.0	VUS	-	0	N		

[a] RefSeq transcript #; *ALG9*, NM_024740; *BBS2*, NM_031885; *CEP290*, NM_025114; *COL4A1*, NM_001845; *DYNC2H1*, NM_001080463; *DZIP1L*, NM_173543; *IFT43*, NM_052873; *OFD1*, NM_003611; *PKD1*, NM_001009944; *PKD2*, NM_000297; *PKHD1*, NM_138694; *TMEM231*, NM_001077416; *TMEM260*, NM_017799; *TTC21B*, NM_024753; *WDR35*, NM_001006657; *WDR60*, NM_018051; [b] FS del, frameshift deletion; Nons, nonsense; Mis, missense; FS dup, frameshift duplication; [c] Non Trunc, nontruncating; [d] NA, not applicable; higher scores indicate a higher probability of pathogenicity; [e] ACMG Des, Designation; P, pathogenic; LP, likely pathogenic, VUS, variant of uncertain significance; LB, likely benign; B, benign; [R], designation associated with biallelic status; [f] the ADPKD Mutation Database: VUS, variant of uncertain significance; M, possible modifying allele; LN, likely neutral.

Figure 1

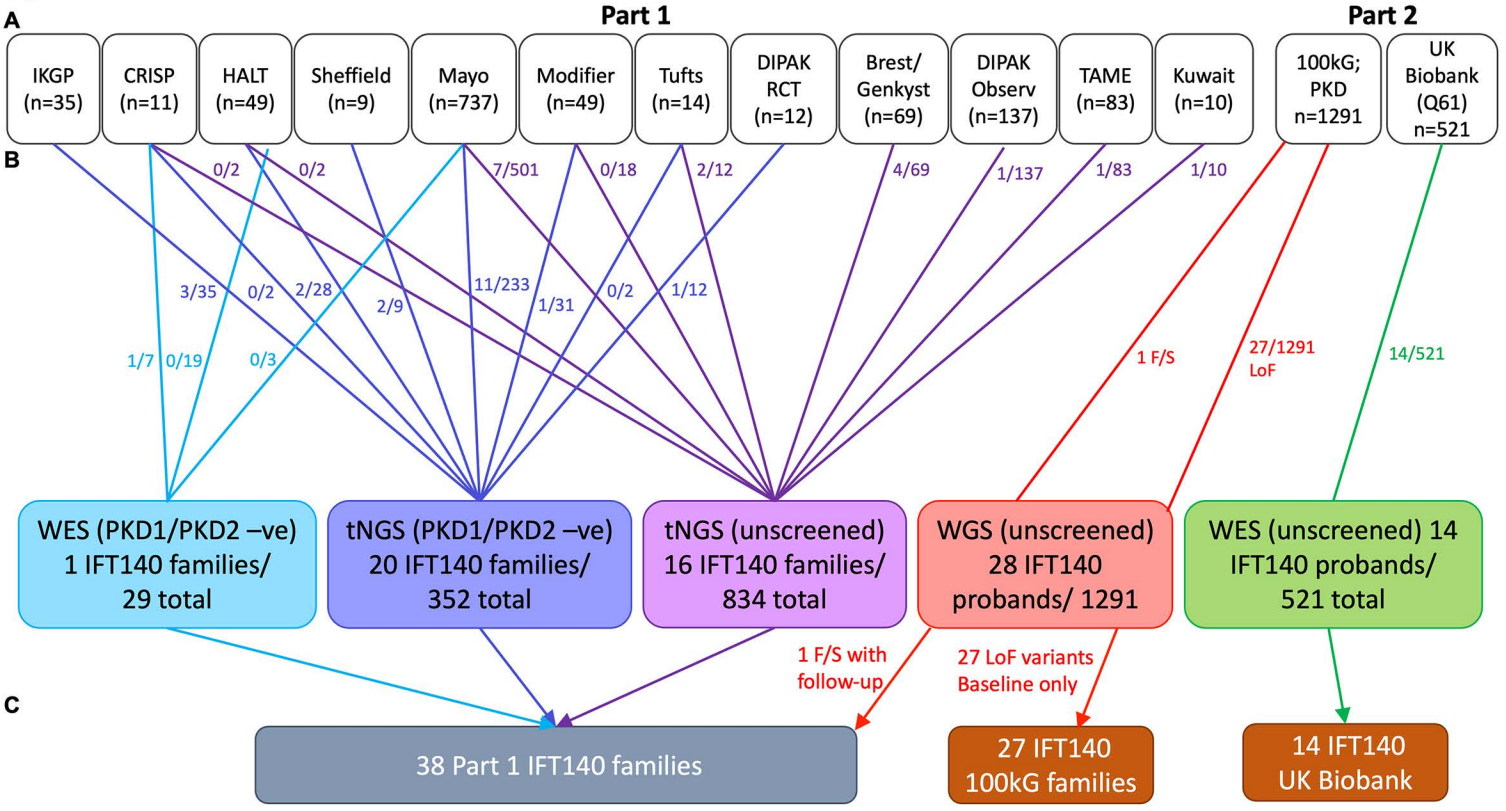
A
Part 1
Part 2
IKGP (n=35)
CRISP (n=11)
HALT (n=49)
Sheffield (n=9)
Mayo (n=737)
Modifier (n=49)
Tufts (n=14)
DIPAK RCT (n=12)
Brest/ Genkyst (n=69)
DIPAK Observ (n=137)
TAME (n=83)
Kuwait (n=10)
100kG; PKD n=1291
UK Biobank (Q61) n=521
B
0/2
0/2
7/501
0/18
2/12
4/69
1/137
1/83
1/10
3/35
0/2
2/28
2/9
11/233
1/31
0/2
1/12
1/7
0/19
0/3
1 F/S
27/1291 LoF
14/521
WES (PKD1/PKD2 –ve) 1 IFT140 families/ 29 total
tNGS (PKD1/PKD2 –ve) 20 IFT140 families/ 352 total
tNGS (unscreened) 16 IFT140 families/ 834 total
WGS (unscreened) 28 IFT140 probands/ 1291
WES (unscreened) 14 IFT140 probands/ 521 total
1 F/S with follow-up
27 LoF variants Baseline only
C
38 Part 1 IFT140 families
27 IFT140 100kG families
14 IFT140 UK Biobank

Figure 2

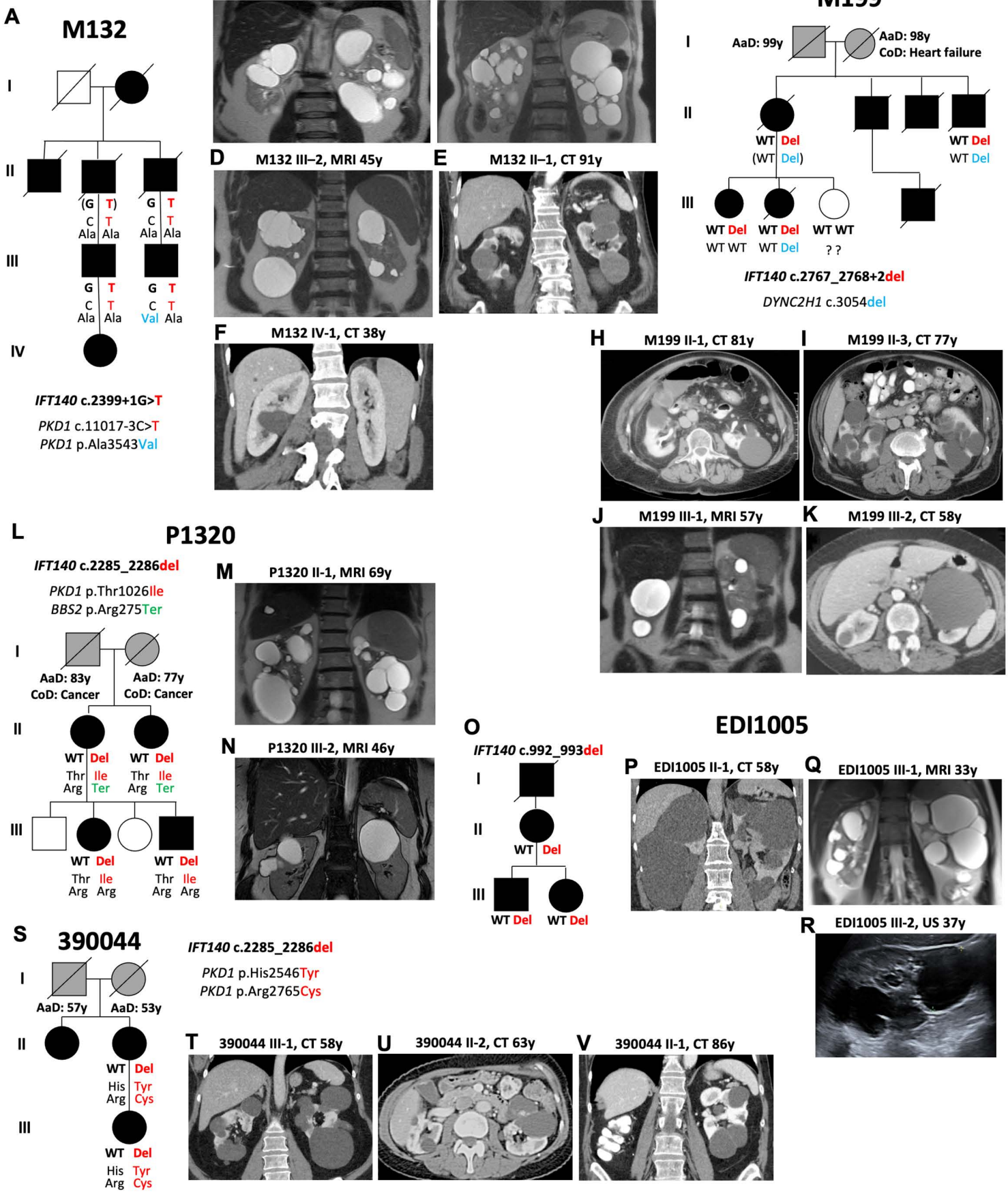
A
M132
I
II
III
IV
(G T)
C T
Ala Ala
G T
C T
Ala Ala
G T
C T
Val Ala
IFT140 c.2399+1G>T
PKD1 c.11017-3C>T
PKD1 p.Ala3543Val
B
M132 II–3, MRI 69y
C
M132 III–1, MRI 63y
D
M132 III–2, MRI 45y
E
M132 II–1, CT 91y
F
M132 IV-1, CT 38y
G
M199
AaD: 99y
AaD: 98y
CoD: Heart failure
WT Del
(WT Del)
WT Del
WT Del
WT Del
WT WT
WT Del
WT Del
WT WT
? ?
IFT140 c.2767_2768+2del
DYNC2H1 c.3054del
H
M199 II-1, CT 81y
I
M199 II-3, CT 77y
J
M199 III-1, MRI 57y
K
M199 III-2, CT 58y
L
P1320
IFT140 c.2285_2286del
PKD1 p.Thr1026Ile
BBS2 p.Arg275Ter
AaD: 83y
CoD: Cancer
AaD: 77y
CoD: Cancer
WT Del
Thr Ile
Arg Ter
WT Del
Thr Ile
Arg Ter
WT Del
Thr Ile
Arg Arg
WT Del
Thr Ile
Arg Arg
M
P1320 II-1, MRI 69y
N
P1320 III-2, MRI 46y
O
IFT140 c.992_993del
WT Del
WT Del
WT Del
EDI1005
P
EDI1005 II-1, CT 58y
Q
EDI1005 III-1, MRI 33y
R
EDI1005 III-2, US 37y
S
390044
AaD: 57y
AaD: 53y
WT Del
His Tyr
Arg Cys
WT Del
His Tyr
Arg Cys
IFT140 c.2285_2286del
PKD1 p.His2546Tyr
PKD1 p.Arg2765Cys
T
390044 III-1, CT 58y
U
390044 II-2, CT 63y
V
390044 II-1, CT 86y

Figure 3

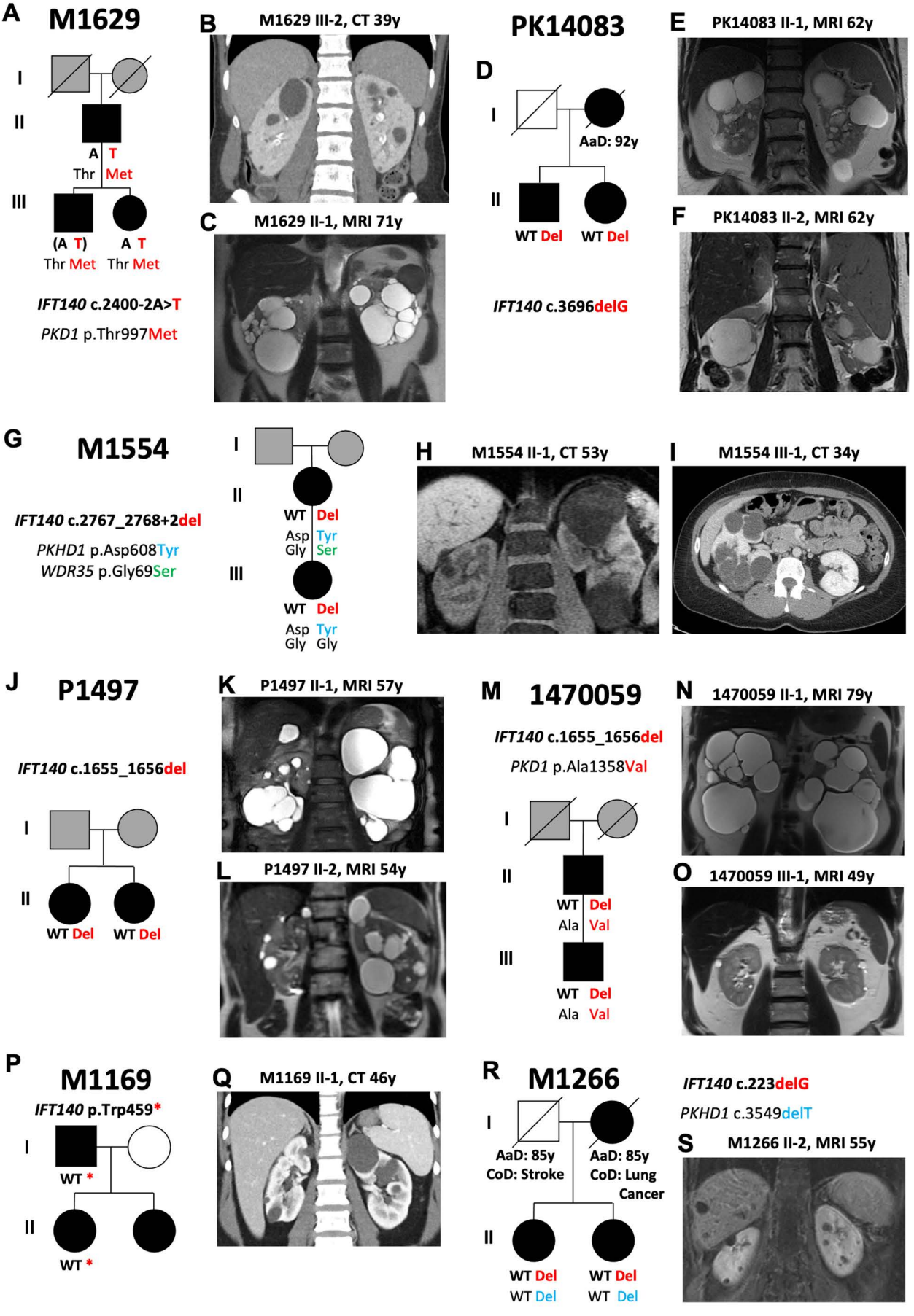
A
M1629
I
II
A T
Thr Met
III
(A T) A T
Thr Met Thr Met
IFT140 c.2400-2A>T
PKD1 p.Thr997Met
B
M1629 III-2, CT 39y
C
M1629 II-1, MRI 71y
PK14083
D
I
AaD: 92y
II
WT Del WT Del
IFT140 c.3696delG
E
PK14083 II-1, MRI 62y
F
PK14083 II-2, MRI 62y
G
M1554
IFT140 c.2767_2768+2del
PKHD1 p.Asp608Tyr
WDR35 p.Gly69Ser
I
II
WT Del
Asp Tyr
Gly Ser
III
WT Del
Asp Tyr
Gly Gly
H
M1554 II-1, CT 53y
I
M1554 III-1, CT 34y
J
P1497
IFT140 c.1655_1656del
I
II
WT Del WT Del
K
P1497 II-1, MRI 57y
L
P1497 II-2, MRI 54y
M
1470059
IFT140 c.1655_1656del
PKD1 p.Ala1358Val
I
II
WT Del
Ala Val
III
WT Del
Ala Val
N
1470059 II-1, MRI 79y
O
1470059 III-1, MRI 49y
P
M1169
IFT140 p.Trp459*
I
WT *
II
WT *
Q
M1169 II-1, CT 46y
R
M1266
I
AaD: 85y
CoD: Stroke
AaD: 85y
CoD: Lung Cancer
II
WT Del WT Del
WT Del WT Del
IFT140 c.223delG
PKHD1 c.3549delT
S
M1266 II-2, MRI 55y

Figure 4

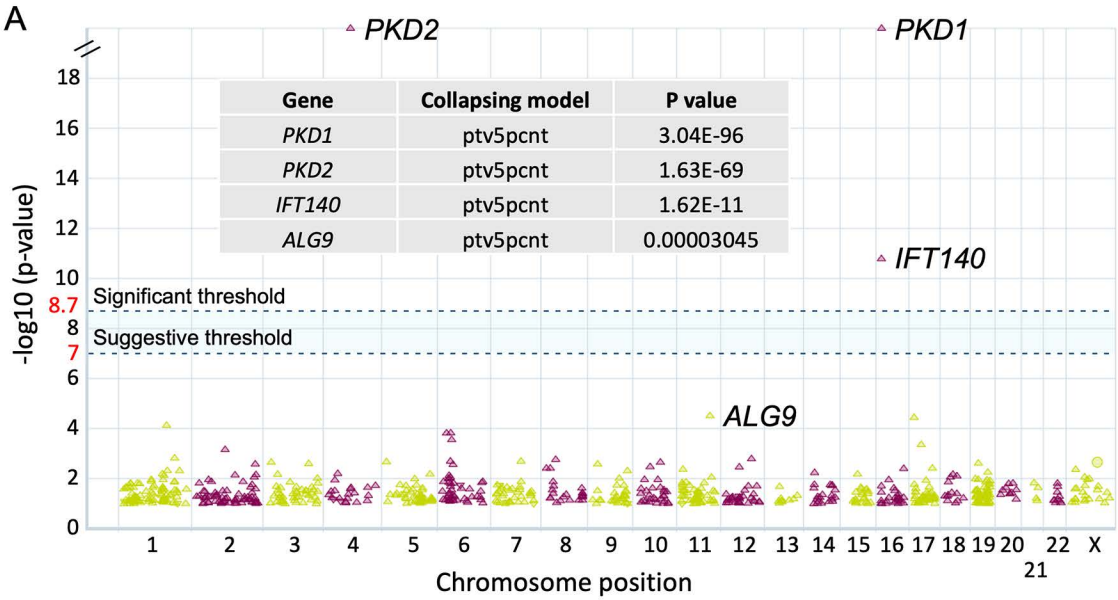

Gene	Collapsing model	P value
PKD1	ptv5pcnt	3.04E-96
PKD2	ptv5pcnt	1.63E-69
IFT140	ptv5pcnt	1.62E-11
ALG9	ptv5pcnt	0.00003045

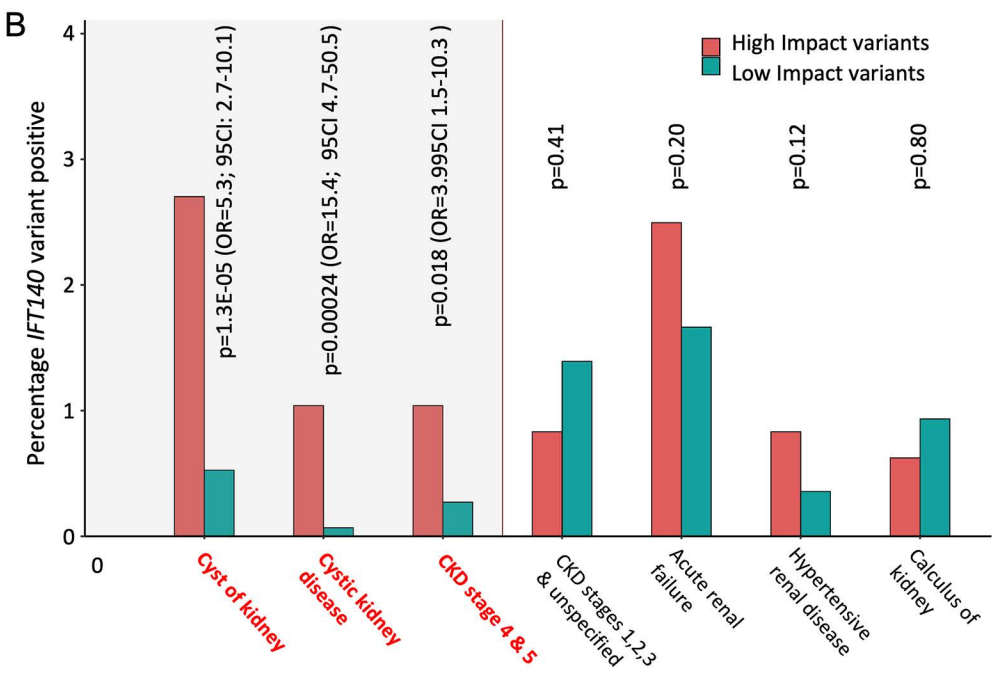

Figure 5

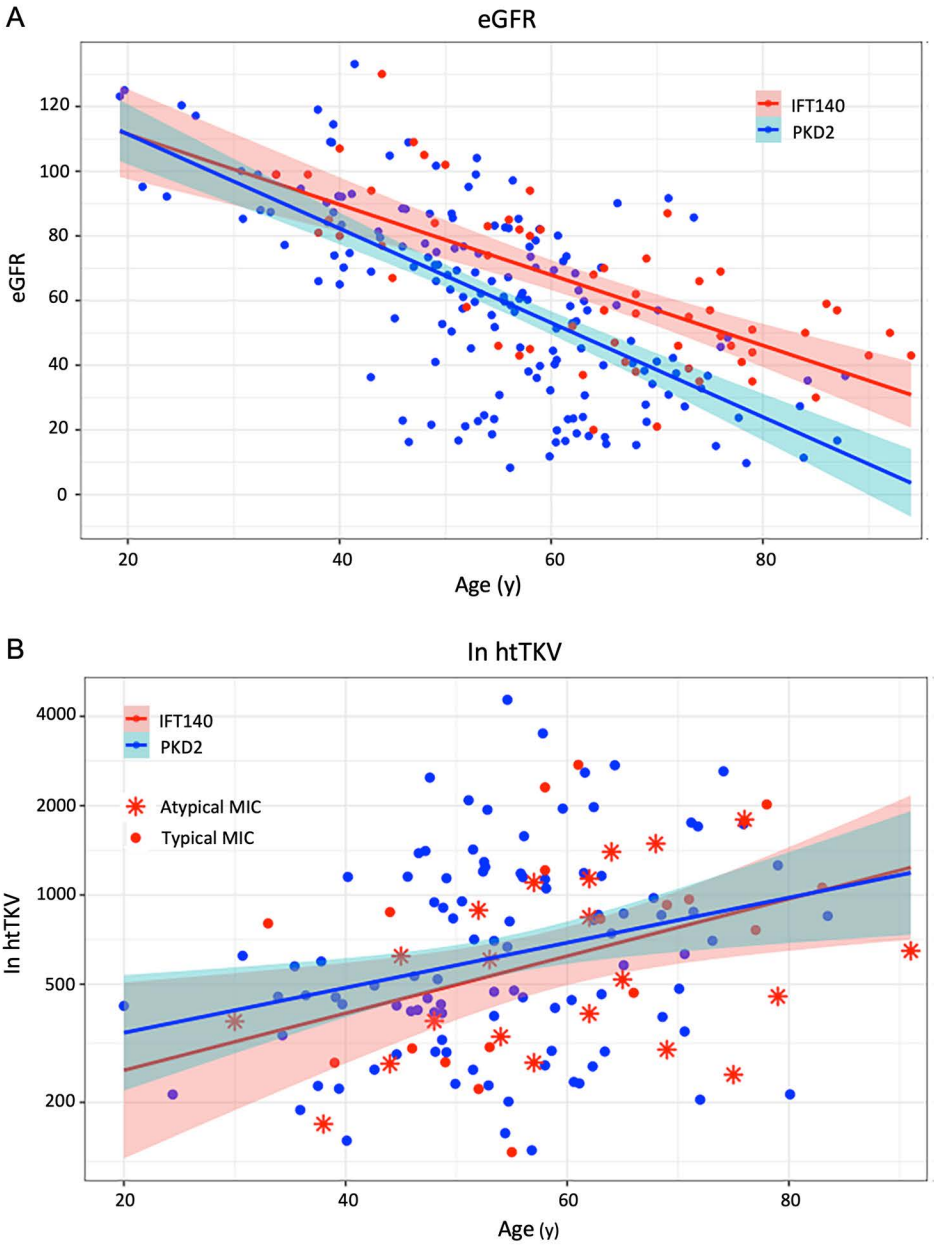
A
eGFR
IFT140
PKD2
eGFR
120
100
80
60
40
20
0
20
40
60
80
Age (y)
B
ln htTKV
IFT140
PKD2
Atypical MIC
Typical MIC
ln htTKV
4000
2000
1000
500
200
20
40
60
80
Age (y)

SUPPLEMENTAL MATERIAL

SUPPLEMENTAL TABLES

Table S1: Primer sets for *IFT140* variant confirmation and segregation

IFT140 Exon	M13 tagged forward primer	M13 tagged reverse primer
Exon 03	GTAAAACGACGGCCAGTCAGTCCGCAAGGCATTT	CAGGAAACAGCTATGACCATGAGCCAGAAGCTACCA
Exon 04	GTAAAACGACGGCCAGTGTAGAGACGGAGTTTCACCAAA	CAGGAAACAGCTATGACCGTTAAGAAGCCCTGAGCTAGAC
Exon 05	GTAAAACGACGGCCAGTGTACCTTGCCAGCCTTCAT	CAGGAAACAGCTATGACCGATTCTTCTGCCACTCCTACAG
Exon 06	GTAAAACGACGGCCAGTACGTGGTGTTGGGTCTTT	CAGGAAACAGCTATGACCCTGCTGCTATCACCGTTACT
Exon 07	GTAAAACGACGGCCAGTTGGATGAGAAGGGCAAGA	CAGGAAACAGCTATGACCAGAGAAAGGGCCGTCAA
Exon 08	GTAAAACGACGGCCAGTCCACCTCACAGAGTTTCTATC	CAGGAAACAGCTATGACCGAATGGGTACGTCCAGTATG
Exon 09	GTAAAACGACGGCCAGTTATCGGCAACGGCTTTCTT	CAGGAAACAGCTATGACCCACCATCACACCTGGCTAAT
Exon 10	GTAAAACGACGGCCAGTGGGCTGATGCTTTGAAGA	CAGGAAACAGCTATGACCCCAAAGTGCTGGGATTACA
Exon 11	GTAAAACGACGGCCAGTAAGTCCGGAACAATGGTACTT	CAGGAAACAGCTATGACCGAACTGAGAGTGGCCTAACC
Exon 12	GTAAAACGACGGCCAGTCAGCAGTGTTCAGAAGTGTTTAG	CGGAAACAGCTATGACCCTCATTAGGCAGGGAGGAAAT
Exon 14	GTAAAACGACGGCCAGTAACACTGAGCGAGTGAATG	CAGGAAACAGCTATGACCAGGAGTCTTCTGGCTTCTAA
Exon 15	GTAAAACGACGGCCAGTAGCTGTGCAGCACTCATC	CAGGAAACAGCTATGACCAAGGTGGGAGGGAGAGAC
Exon 16	GTAAAACGACGGCCAGTGGGTGTGTTTCTCTTGACAT	CAGGAAACAGCTATGACCTGAAGGCGCGTTAACTTAG
Exon 17	GTAAAACGACGGCCAGTAAGTTCTCCCAGAGCTGA	CAGGAAACAGCTATGACCAGAGACGAGGGTCTCAATA
Exon 19	GTAAAACGACGGCCAGTGACTGGGCCTGTTGGTAAATA	CAGGAAACAGCTATGACCCGCAGTCATGAGGAGTCAAA
Exon 20	GTAAAACGACGGCCAGTCCGCTTAGAGCAGGGAAA	CAGGAAACAGCTATGACCACATCAGTGCAGGCTCAG
Exon 21	GTAAAACGACGGCCAGTTTTGAGACGTGGGTGTGTG	CAGGAAACAGCTATGACCATCTCCGAGACTGGGAGAAG
Exon 22	GTAAAACGACGGCCAGTCCGCTCTGATGCGTTT	CAGGAAACAGCTATGACCCAGGAAGCACGGGAAAG
Exons 23-24	GTAAAACGACGGCCAGTCAGGTGACATGCACTCTAAG	CAGGAAACAGCTATGACCCACTGACACGATTCTCTCTG
Exon 26	GTAAAACGACGGCCAGTCCCGATACTACGAGGAGAA	CAGGAAACAGCTATGACCCCTTCCTGGAGAACTCATAAC
Exon 27	GTAAAACGACGGCCAGTGCGTGAGAAAGTAACGTGAATG	CAGGAAACAGCTATGACCCCCGGTAGAGAGAGATCTTAGT
Exon 28	GTAAAACGACGGCCAGTCCCTGAGCCACTCTTCTT	CAGGAAACAGCTATGACCGCTTTGTCGTAGTTCTGGTATT
Exon 29	GTAAAACGACGGCCAGTAGAACATCATCGGCTTCTACAC	CAGGAAACAGCTATGACCTGTTTCCAGAACACCTTCCC
Exon 30	GTAAAACGACGGCCAGTGTCTCCTCTGACCTCTGATAG	CAGGAAACAGCTATGACCCCCAAAGTGCTGGGATTAC
Exon 31	GTAAAACGACGGCCAGTCCATCACCAATGGGAAGC	CAGGAAACAGCTATGACCGGCCCTGCAGGAGTAT

Table S2: Genetic and other phenotypic details of individuals with *IFT140* pathogenic variants

Pedigree (Study)[a]	Pathogenic *IFT140* variant	Subject[b]	Other conditions[e]	Other family member information[f]
Families				
M132 (Mayo)	c.2399+1G>T (p.Ser800?)	I-2[c]	†97y, stroke	
		II-1[c]	AMD, †94y, multiple TIA	
		II-2[d]	DV, hernia, †81y, AD	
		II-3	†74y, lung adenocarcinoma	
		III-1	Bladder cancer,	
		III-2	Arthritis	
		IV-1[c]	Ovarian cysts	
M199 (Mayo)	c.2767_2768+2del (p.Tyr923fs*18)	II-1	AD, †87y, stroke	
		II-2[c]	2DM, DV, †72y, stroke	
		II-3[c]	†80y, prostate cancer	
		II-4	2DM, AAA, †78y, ?	
		III-1	AMD	
		III-2	EO SHL, SC, †71y, COPD	
		III-4	†72y sepsis, 2DM, CC, CHTF, DV, LCir, PHT, SM	
P1320 (Shef)	c.2285_2286del (p.Phe762fs*39)	II-1	MI, 42y	
		II-2	NL, hernia	
		III-2	-	
		III-4	-	
EDI1005 (100kG)	c.992_993del (p.Cys331fs*3)	I-1[c]	†89y, ?	
		II-1	Ovarian cysts	
		III-1	-	
		III-2	Ovarian cysts	
390044 (HALT)	c.2483delG (p.Gly828fs*18)	II-1[c]	CC	
		II-2	Melanoma	
		III-1	CC, lung cancer	
M1629 (Mayo)	c.2400-2A>T (p.Ser800?)	II-1	MH, proteinuria, HypT	
		III-1	-	
		III-2	MH	
PK14083 (Brest)	c.3696delG (p.Ile1234fs*33)	II-1	2DM (55), sleep apnea	Mother (†92y) PKD w/o ESKD
		II-2	Gout, polycythemia vera	
M1554 (Tufts)	c.2767_2768+2del (p.Tyr923*18)	II-1	Ovarian cyst	
		III-1	-	
P1497 (DIPAK^{R})	c.1655_1656del (p.Glu552fs*6)	II-1	-	
		II-2	-	
1470059 (Mod)	c.1655_1656del (p.Glu552fs*6)	II-1	SHL, cataracts, HypT	
		III-1	-	
M1169 (Mayo)	c.1377G>A (p.Trp459*)	I-1		Daughter II-2: 3 RK, 2 LK cysts
		II-1	IA, NL, hernia	
M1266 (Mayo)	c.223delG (p.Val75fs*11)	II-1	NL, Fatty liver, cholelithiasis	
		II-2	NL, EO SHL;	Mother (†85y) PKD, IA

Pedigree (Study)[a]	Pathogenic *IFT140* variant	Subject[b]	Other conditions[e]	Other family member information[f]
Singletons				
440003 (CRISP)	c.581delT (p.Leu194fs*2)	406737	2DM, SLE	Brother, 1 K cyst
690036 (HALT)	c.931dupT (p.Tyr311fs*7)	E4669644		Mother (85y) PKD w/o ESKD; Grandmother, PKD (†77y) w/o ESKD
F430 (Dublin)	c.2278C>T (p.Arg760*)	8143		Sister PKD, CKD1
F392 (Dublin)	c.490G>T (p.Glu164*)	10235	MH	Sister & Daughter IFT140 +ve but -ve US, 53y & 40y
F662 (Dublin)	c.1010-1G>A (p.Gly337?)	10664	Retinal detachment	F/H Ukn
M120 (Mayo)	c.2909_2920del (p.Glu970_Ala973del)	R1097	Degenerative disc disease	Mo (†82y) Kidney cysts
M154 (Mayo)	c.2399+1G>T (p.Ser800?)	R1142	Junctional tachycardia	PKD F/H Ukn
M187 (Mayo)	c.2399+1G>T (p.Ser800?)	R19	DV, RS, (†85y) CC	PKD F/H Unk
M241 (Mayo)	c.1377G>A (p.Trp459*)	R1403	HCM	F/H Ukn, Son IFT140 +ve but no info
M274 (Mayo)	c.1377G>A (p.Trp459*)	R1367	MI, lamellar macular hole	PKD F/H Ukn
M323 (Mayo)	c.2399+1G>T (p.Ser800?)	R1606	2DM, AAA, (†79y) ?	PKD F/H Ukn
M357 (Mayo)	c.2399+1G>T (p.Ser800?)	R874	DV, (†79y) MM	Mother 1 Lg cyst, F/H CC
M614 (Mayo)	c.490G>T (p.Glu164*)	R1942	NL, DV	PKD F/H Ukn
M1062 (Mayo)	c.2767_2768+2del (p.Tyr923fs*18)	R2939	Macular fibrosis, retinal detachment	PKD F/H Ukn
M1111 (Mayo)	c.1653-1G>A (p.Arg551?)	R2995	Lung cancer, DV	PKD F/H Ukn, F/H CC
M1261 (Tufts)	c.490G>T (p.Glu164*)	R3221	ADHD, depression	Father (67y) +ve PKD, F/H CC
M1277 (Mayo)	c.634G>A (p.Gly212?)	R3248	Leukopenia, WT, 6mo	
M1374 (Mayo)	c.594dupG (p.Ser199fs*21)	R3376	Celiac, AMD	Parents (†93y) (†91y) PKD Ukn, Father AMD
M1540 (Mayo)	c.1565G>A (p.Gly522Glu)	R2098	CC, DV, IA, (†85y) ?	
P1195 (Shef)	c.2399+1G>T (p.Ser800?)	Ox3922	(†92y) RTI	Brother PKD, AAA (†84y)
P1480 (Kuw)	c.1525-1G>A (Gly509?)	Ox5181		F/H Ukn
P1504 (DIPAK^{O})	c.2399+1G>T (p.Ser800?)	Ox5058		Father ESKD 80y, Brother CKD
P1505 (TAME)	c.1377G>A (p.Trp459*)	Ox5262	CA, blindness, 4mm IA	
PK14084 (Genkyst)	c.2542_2559del (p.Arg848_Ala853del)	210192		
PK14082 (Brest)	c.1010-1G>A (p.Gly337?)	200138	Aortic dilatation	
PK14085 (Brest)	c.1648C>T (p.Arg550*)	210193	Degenerative disc disease, chronic headache	

[a] DIPAK^{R}**,** DIPAK randomized clinical trial; 100kG, 100,000 Genomes; Kuw, Kuwait; Mod, Modifiers of PKD Study; Shef, Sheffield; DIPAK^{O}, DIPAK Observational Study; [b, c]no sample for genetic confirmation; [d]genotype inferred; [e] †, age and cause of death; +ve, positive; -ve, negative; 2DM, type 2 diabetes mellitus; AAA, abdominal aortic aneurysm; AD; Alzheimer's Disease; ADHD, attention deficit hyperactivity disorder; AMD, age-related macular degeneration; CA, congenital aniridia; CC, colorectal cancer; CHTF, congestive heart failure; COPD, Chronic obstructive pulmonary disease; DV, diverticulosis; EO, early onset; HCM, hypertrophic cardiomyopathy; HypT, hypothyroidism; IA, intracranial aneurysm; LCir, Liver Cirrhosis; MI, myocardial infarction; MM, multiple myeloma; NL, nephrolithiasis; PHT, portal hypertension; RS, retinal sclerosis; RTI, respiratory tract infection; SC, splenic cysts; SHL, sensorineural hearing loss; SLE, systemic lupus erythematosus; SM, splenomegaly; TIA, transient ischemic attack; w/o, without; WT, Wilms tumor; [f] AMD, age-related macular degeneration; CC, colorectal cancer; ESKD, end stage kidney disease; F/H, family history; IA, intracranial aneurysm; LK, left kidney; PKD, polycystic kidney disease; RK, right kidney; Ukn, unknown.

Table S3: Details of individuals with *IFT140* pathogenic variants in the 100K Genomes Cystic Kidney Disease Cohort

Pedigree	cDNA change	Protein Change	Subject	Sex	Age	HTN	Relationship	Family history	Kidney Phenotype	Liver Phenotype	Other Conditions/Information[a]
Families											
UK1	c.2278C>T	p.Arg760*	UK1-1	M	57	Y	Proband	Affected sons	Multiple cysts	NA	Hematuria
			UK1-3	M	27	NA	Son	Affected father	PKD	NA	Inguinal hernia
			UK1-2	M	30	NA	Son	Affected father	PKD	NA	-
UK2	c.2399+1G>T	p.Ser800?	UK2-1	M	49	NA	Proband	Mother, sibs affected	Multiple small medullary cysts	Y	Carotid paraganglioma
			UK2-2	F	76	Y	Mother	Affected son	Multiple cysts	Y	-
			UK2-4	F	52	NA	Sister	Affected mother	Multiple cysts	NA	Carotid paraganglioma
			UK2-3	F	51	Y	Sister	Affected mother	Multiple cysts	NA	Paraganglioma
UK3	c.2399+1G>T	p.Ser800?	UK3-1	M	19	Y	Proband	Affected father	Multiple cortical cysts	NA	-
			UK3-2	M	49	NA	Father	Affected son	Multiple cortical cysts	NA	-
Singletons											
UK4	c.1147C>T	p.Gln383*	UK4-1	M	68	Y	Proband	Unknown	Multiple cysts	NA	Diaphragmatic hernia
UK5	c.3214C>T	p.Arg1072*	UK5-1	M	64	Y	Proband	Affected mother	Multiple cysts, CKD	NA	Ischemic heart disease, hematuria
UK6	c.2399+1G>T	p.Ser800?	UK6-1	F	61	Y	Proband	Unknown	Multiple cysts	NA	Diverticular disease, dilation cerebral artery, PCOS
UK7	c.2399+1G>T	p.Ser800?	UK7-1	M	47	NA	Proband	Affected father	Multiple cysts	NA	-
UK8	c.2500C>T	p.Arg834*	UK8-1	M	48	NA	Proband	Mother, 2 sibs affected	Multiple cysts	NA	-
UK9	c.1648C>T	p.Arg550*	UK9-1	M	52	NA	Proband	Parents unaffected	Multiple cortical cysts	NA	-
UK10	c.1246C>T	p.Gln416*	UK10-1	M	70	Y	Proband	Unknown	Multiple glomerular cysts, CKD	NA	Gout, heart abnormalities
UK11	c.1039C>T	p.Arg347*	UK11-1	F	53	NA	Proband	Affected mother	Cystic kidney disease	NA	Hematuria
UK12	c.1377G>A	p.Trp459*	UK12-1	M	63	Y	Proband	Parents unaffected	Multiple glomerular cysts, CKD3	NA	Diverticular disease, hematuria, neoplasia
UK13	c.1959G>A	p.Trp653*	UK13-1	M	84	Y	Proband	Parents unaffected	Multiple cysts, CKD3	NA	Ischemic heart disease, diaphragmatic hernia, neoplasia
UK14	c.1377G>A	p.Trp459*	UK14-1	M	58	Y	Proband	Unknown	Multiple cysts	NA	-
UK15	c.2399+1G>T	p.Ser800?	UK15-1	F	48	NA	Proband	Affected father	Multiple cysts, kidneys enlarged, CKD	NA	-
UK16	c.1359+1G>A	p.Lys453?	UK16-1	M	8	NA	Proband	Parents unaffected	Multiple glomerular & small medullary cysts	NA	preaxial foot polydactyly, polyhydramnios
UK17	c.1246C>T	p.Gln416*	UK17-1	M	17	NA	Proband	Parents unaffected	Multiple small medullary & cortical cysts	NA	Ehlers Danlos syndrome
UK18	c.2399+1G>T	p.Ser800?	UK18-1	M	22	NA	Proband	Parents unaffected	Multiple cysts	NA	-
UK19	c.2399+1G>T	p.Ser800?	UK19-1	M	49	Y	Proband	Affected father	Multiple cysts	NA	Diaphragmatic hernia
UK20	c.2998-1G>A	p.Lys999?	UK20-1	M	86	NA	Proband	Unknown	Multiple cysts	NA	-
UK21	c.2399+1G>T	p.Ser800?	UK21-1	F	38	NA	Proband	Affected mother	Multiple small medullary cysts	NA	Neoplasia, PCOS
UK22	c.2399+1G>T	p.Ser800?	UK22-1	M	77	NA	Proband	Parents unaffected	Multiple cysts	NA	Bladder neoplasm, polycythemia vera
UK23	c.2399+1G>T	p.Ser800?	UK23-1	M	56	Y	Proband	Parents unaffected	Multiple cysts	NA	-
UK24	c.2399+1G>T	p.Ser800?	UK24-1	F	61	Y	Proband	Parents unaffected	Multiple cysts	NA	Endometrial carcinoma, diaphragmatic hernia
UK25	c.810+1G>A	p.Lys270?	UK25-1	M	67	Y	Proband	Parents unaffected	Multiple cysts	NA	Diverticular disease

Pedigree	cDNA change	Protein Change	Subject	Sex	Age	HTN	Relationship	Family history	Kidney Phenotype	Liver Phenotype	Other Conditions/Information[a]
UK26	c.1377G>A	p.Trp459*	UK26-1	M	67	N	Proband	Father & sib affected	Multiple cortical cysts, enlarged kidneys	Y	Ischemic heart disease
UK27	c.2399+1G>T	p.Ser800?	UK27-1	M	60	Y	Proband	Unknown	Multiple cysts, CKD1	NA	Schwannoma, DM Type 2

[a] PCOS; polycystic ovary syndrome; DM Type 2, type 2 diabetes

SUPPLEMENTAL FIGURES

Figure S1

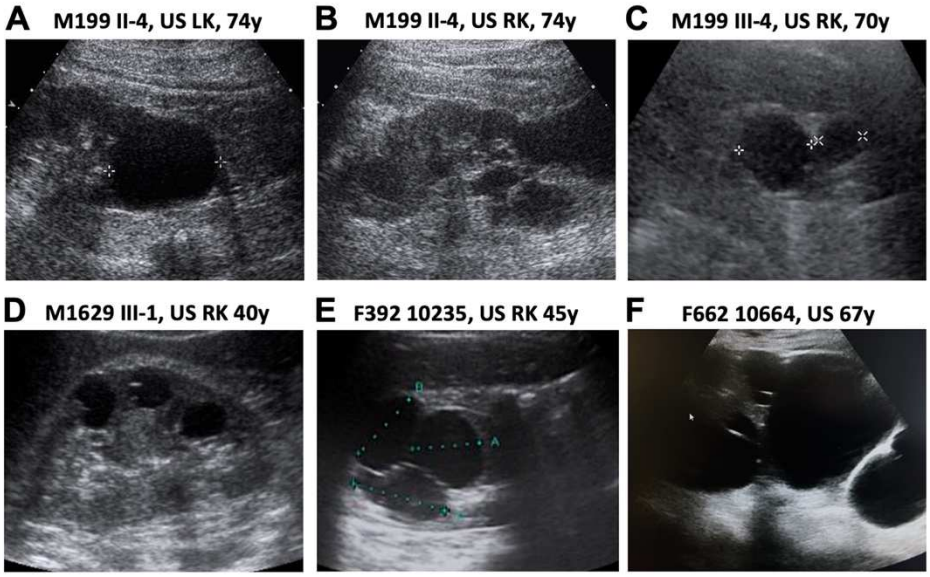

Figure S1. Ultrasound images of IFT140 subjects' kidneys. Images of members of families M199 (**A**-**C**), M1629 (**D**), F392 (**E**) and F662 (**F**). The cystic kidney disease usually consists of a few large cysts.

Figure S2

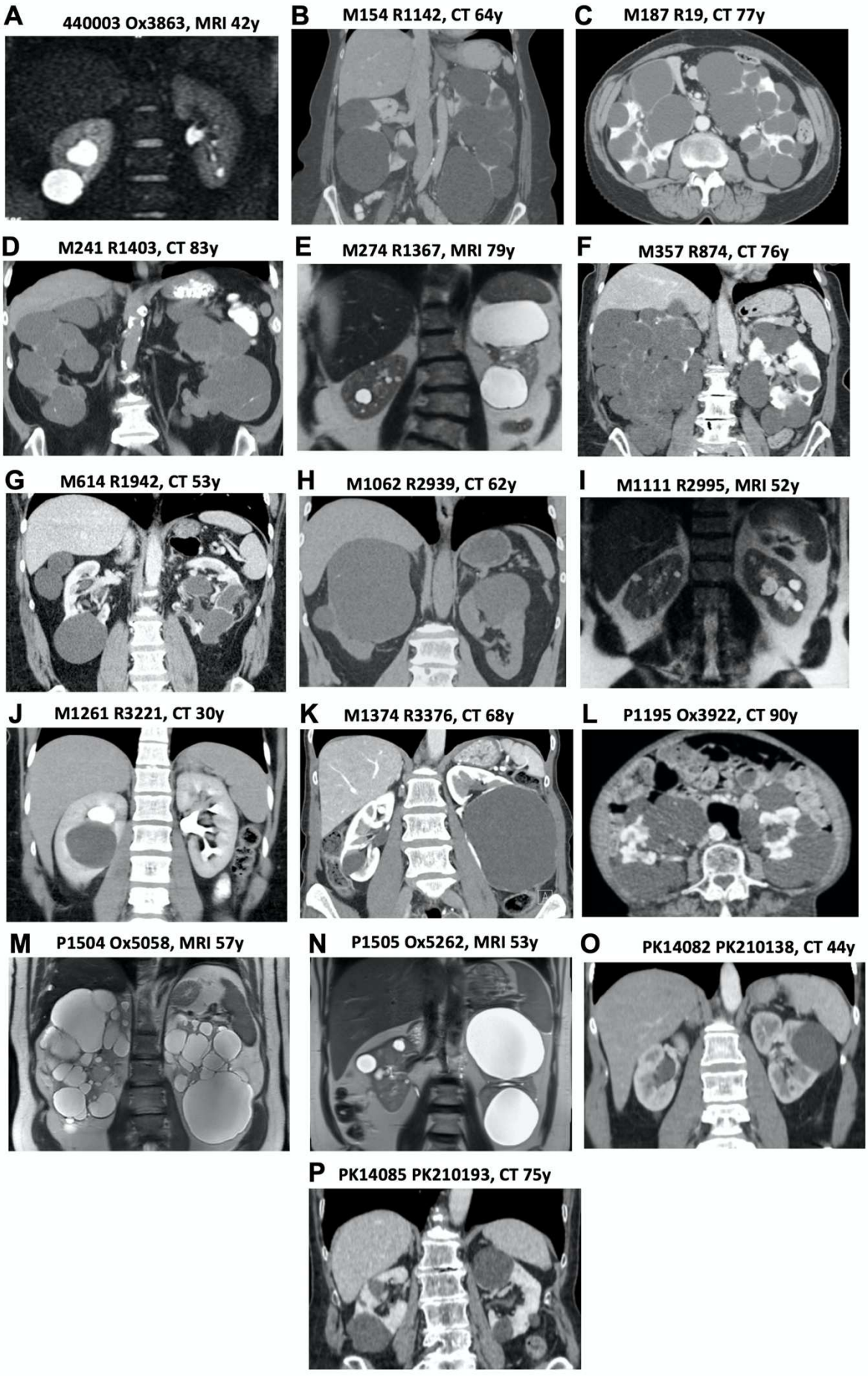
A
440003 Ox3863, MRI 42y
B
M154 R1142, CT 64y
C
M187 R19, CT 77y
D
M241 R1403, CT 83y
E
M274 R1367, MRI 79y
F
M357 R874, CT 76y
G
M614 R1942, CT 53y
H
M1062 R2939, CT 62y
I
M1111 R2995, MRI 52y
J
M1261 R3221, CT 30y
K
M1374 R3376, CT 68y
L
P1195 Ox3922, CT 90y
M
P1504 Ox5058, MRI 57y
N
P1505 Ox5262, MRI 53y
O
PK14082 PK210138, CT 44y
P
PK14085 PK210193, CT 75y

Figure S2: Kidney and liver images of 16 singleton subjects with *IFT140* pathogenic variants. Coronal MRI (**A**, **E**, **I**, **M**, **N**), or CT (**B**, **D**, **F**-**H**, **J**, **K**, **O**, **P**), or axial CT (**C**, **L**) images showing the kidney and liver phenotype. A range of variability in terms of severity is seen between very cystic (for example **D**, **F**, **M**) to much more mildly affected (for example **A**, **I**, **J**).

Figure S3

A

***IFT140* c.634G>A (p.Gly212Arg)**

M1277 R3248, CT 61y

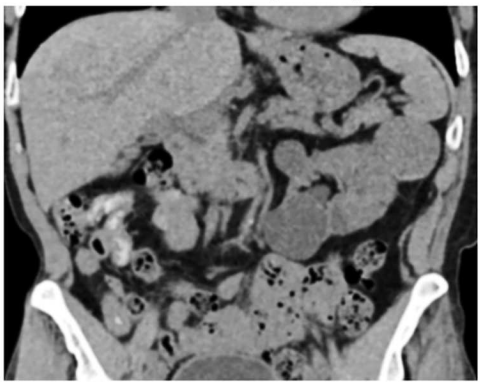

R nephrectomy - Wilm's Tumor

B

EX4 | IVS4

5'-...GATGGAC A/G | GTGAGG...-3'

BDGP Score: 0.93 → 0.08

C

							R						
Human	206	F	V	S	L	M	D	G	T	V	H	Y	V	D	220
Mouse	206	F	V	S	L	M	D	G	T	V	H	Y	V	D	220
Rat	206	F	V	S	L	M	D	G	T	V	H	Y	V	D	220
Bovine	206	F	V	S	L	T	D	G	T	V	H	H	V	D	220
Chicken	206	F	I	T	L	T	D	G	S	V	H	Y	V	N	220
Zebrafish	207	Y	I	S	T	A	D	G	S	V	Y	S	V	D	221
Frog	206	F	L	S	A	K	D	G	S	V	Y	F	V	N	220
FruitFly	211	Y	A	C	T	Q	G	G	V	V	Y	Y	I	N	225
Mosquito	211	Y	A	C	T	Q	A	G	I	L	Y	Y	I	N	225
Nematode	192	L	F	A	G	K	S	G	T	I	Y	G	V	D	206

D

M1540 R2098, CT 66y

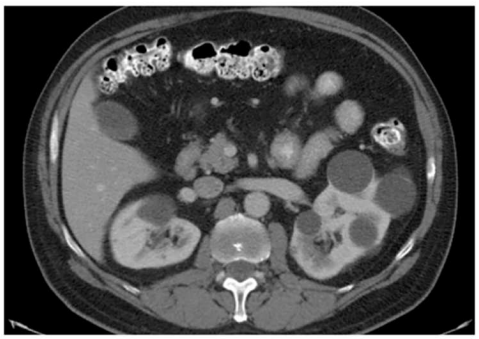

E

***IFT140* c.1565G>A (p.Gly522Glu)**

							E						
Human	516	L	F	S	E	T	E	G	N	P	C	F	L	D	530
Mouse	516	L	F	S	E	T	E	G	S	P	C	F	L	D	530
Rat	516	L	F	S	E	T	E	G	S	P	C	F	L	D	530
Bovine	516	P	F	S	E	S	E	G	N	P	C	F	L	D	530
Chicken	517	V	F	S	E	A	E	G	N	P	C	L	L	D	531
Zebrafish	515	V	F	S	E	A	E	G	N	P	T	L	L	S	529
Frog	517	P	F	S	E	A	E	G	N	P	C	G	L	D	531
FruitFly	590	Q	A	S	D	I	E	G	K	I	I	G	M	D	604
Mosquito	557	V	F	N	A	N	E	G	K	P	I	G	V	D	571
Nematode	497	S	L	P	E	I	E	G	D	P	E	I	L	E	511

F

M120 R1097, MRI 65y

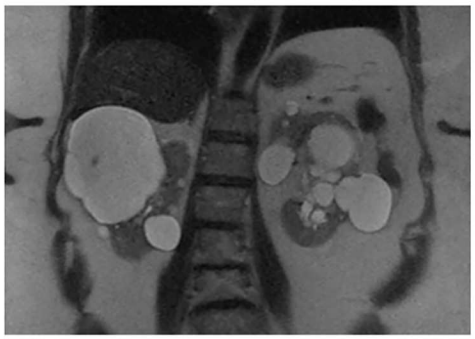

G

***IFT140* p.Glu970_Ala973del**

					-	-	-	-					
Human	966	E	S	Q	G	E	M	D	A	A	L	H	Y	Y	980
Mouse	967	E	S	Q	A	E	M	D	T	A	L	R	Y	Y	981
Rat	979	E	S	Q	A	E	M	D	T	A	L	R	Y	Y	993
Bovine	961	E	S	Q	A	K	M	D	A	A	L	H	Y	Y	975
Chicken	958	E	S	Q	S	D	L	E	S	A	L	K	Y	Y	972
Zebrafish	956	E	S	Q	S	D	M	E	A	A	L	H	Y	Y	970
Frog	966	E	S	Q	S	N	L	D	A	A	L	K	Y	Y	980
FruitFly	1000	E	S	S	G	D	M	D	A	A	L	A	V	Y	1014
Mosquito	986	E	S	S	G	D	M	E	G	A	F	K	I	Y	1000
Nematode	944	E	S	V	G	E	L	E	G	A	I	S	F	Y	958

H

PK14084 PK210192, MRI 48y

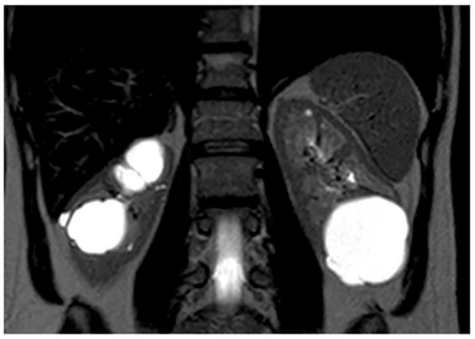

I

***IFT140* p.Arg848_Ala853del**

						-	-	-	-	-			
Human	844	E	L	E	A	R	V	A	V	L	A	T	Q	L	858
Mouse	845	E	L	E	A	R	V	A	M	L	A	I	Q	L	859
Rat	857	E	L	E	A	R	V	A	M	L	A	I	Q	L	871
Bovine	839	E	P	E	A	R	V	A	M	L	A	V	Q	L	853
Chicken	836	E	Q	E	A	R	V	A	V	L	A	V	Q	L	850
Zebrafish	834	E	V	E	A	Q	V	A	V	L	A	T	Q	L	848
Frog	844	E	V	E	A	R	V	A	M	L	A	I	Q	L	858
FruitFly	878	E	T	E	A	K	V	A	V	L	A	I	E	L	892
Mosquito	864	E	Q	E	A	R	V	A	V	L	A	I	E	L	878
Nematode	819	N	D	S	M	K	C	A	A	L	A	I	E	L	833

Figure S3: Genetic and phenotypic details of individuals with inframe *IFT140* pathogenic variants. (A) Abdominal coronal (**A**) or axial (**D**) CT, or coronal MRI (**F**, **H**) imaging with the age at imaging indicated shows the kidney and liver phenotypes. (**B**) *IFT140*: c.634G>A is substitution of the last nucleotide of exon 4 and is significantly predicted to weaken the donor site, details of the Berkeley Drosophila Genome Project (BDGP) Splice Site Prediction by Neural Network are shown (**B**). Multisequence alignments of orthologs from human to nematode worm showing the conservation of the substituted residue (**C**, **E**) or group of deleted residues (**G**, **I**).

Figure S4

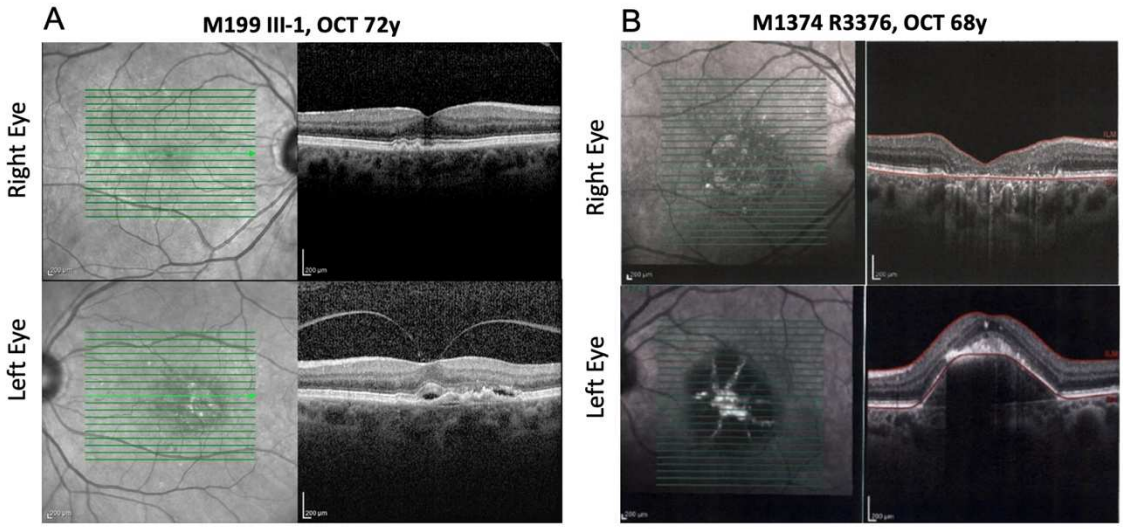

Figure S4: Optical Coherence Tomography imaging of ocular phenotypes in two *IFT140* LoF subjects. (**A**) Bilateral retinal and age-related macular degeneration (AMD) in M199 III-1. The right eye shows drusen, while the left eye shows drusen and accumulation of subretinal fluid with vitreomacular tension and early-stage retinal pigment epithelium (RPE) detachment. (**B**) Bilateral macular changes in R3376. The right eye shows marked atrophy of the RPE. The left eye shows RPE detachment consistent with macular degeneration.

SUPPLEMENTAL ACKNOWLEDGEMENTS

The HALT PKD study was supported by NIDDK cooperative agreements (DK062410, DK062408, DK062402, DK082230, DK062411, and DK062401), and National Center for Research Resources General Clinical Research Centers (RR000039, RR000585, RR000054, RR000051, RR023940, RR001032) and National Center for Advancing Translational Sciences Clinical and Translational Science Awards (RR025008, TR000454, RR024150, TR00135, RR025752, TR001064, RR025780, TR001082, RR025758, TR001102, RR033179, TR000001). The CRISP study was supported by NIDDK grants (DK056943, DK056956, DK056957, DK056961), and the ADPKD Modifier Study was supported by NIDDK grant, DK079856. The Genkyst cohort was supported by National Plans for Clinical Research, Groupement Interregional de Recherche Clinique et d'Innovation (GIRCI Grand Ouest), and the French Society of Nephrology. TAME was supported by Department of Defense contract W81XWH-15-1-0663, by the National Center for Advancing Translational Sciences, National Institutes of Health Award Numbers UL1TR002544 and 1UL1TR003098, The DIPAK Consortium was sponsored by the Dutch Kidney Foundation (grants CP10.12 and CP15.01) and Dutch government (LSHM15018).

The UK Biobank (project ID 43879) is supported by its founding funders the Wellcome Trust and UK Medical Research Council, as well as the Department of Health, Scottish Government, the Northwest Regional Development Agency, British Heart Foundation and Cancer Research UK. The organization has over 150 dedicated members of staff, based in multiple locations across the UK. The AstraZeneca PheWAS Portal is a public repository of gene-phenotype associations. These data were generated using exome sequencing and phenotype data from the UK Biobank accessed as part of application 26041. Association statistics generated in this study are publicly available through our AstraZeneca Centre for Genomics Research (CGR) PheWAS Portal. All whole-exome sequencing data described in this paper are publicly available to registered researchers through the UKB data access protocol. Exomes can be found in the UKB showcase portal.

The 100,000 Genomes Project is managed by Genomics England Limited (a wholly owned company of the Department of Health and Social Care). The 100,000 Genomes Project is funded by the National Institute for Health Research and NHS England. The Wellcome Trust, Cancer Research UK and the Medical Research Council have also funded research infrastructure. The 100,000 Genomes Project uses data provided by affected individuals and collected by the National Health Service as part of their care and support.

The current affiliation of SL is Department of Pathology, Westchester Medical Center, Valhalla, NY.

We acknowledge members of The Genomics England Research Consortium: John C. Ambrose[1]; Prabhu Arumugam[1]; Roel Bevers[1]; Marta Bleda[1] ; Freya Boardman-Pretty[1,2]; Christopher R. Boustred[1]; Helen Brittain[1]; Mark J. Caulfield[1,2]; Georgia C. Chan[1]; Greg Elgar[1,2]; Tom Fowler[1]; Adam Giess[1]; Angela Hamblin[1]; Shirley Henderson[1,2]; Tim J. P. Hubbard[1]; Rob Jackson[1]; Louise J. Jones[1,2]; Dalia Kasperaviciute[1,2]; Melis Kayikci[1]; Athanasios Kousathanas[1]; Lea Lahnstein[1]; Sarah E. A. Leigh[1]; Ivonne U. S. Leong[1]; Javier F. Lopez[1]; Fiona Maleady-Crowe[1]; Meriel McEntagart[1]; Federico Minneci[1]; Loukas Moutsianas[1,2]; Michael Mueller[1,2]; Nirupa Murugaesu[1]; Anna C. Need[1,2]; Peter O'Donovan[1]; Chris A. Odhams[1]; Christine Patch[1,2]; Mariana Buongermino Pereira[1]; Daniel Perez-Gil[1]; John Pullinger[1]; Tahrima Rahim[1]; Augusto Rendon[1]; Tim Rogers[1]; Kevin Savage[1]; Kushmita Sawant[1]; Richard H. Scott[1]; Afshan Siddiq[1]; Alexander Sieghart[1]; Samuel C. Smith[1]; Alona Sosinsky[1,2]; Alexander

Stuckey[1]; Mélanie Tanguy[1]; Ana Lisa Taylor Tavares[1]; Ellen R. A. Thomas[1,2]; Simon R. Thompson[1]; Arianna Tucci[1,2]; Matthew J. Welland[1]; Eleanor Williams[1]; Katarzyna Witkowska[1,2]; Suzanne M. Wood[1,2].

1. Genomics England, London, UK; 2. William Harvey Research Institute, Queen Mary University of London, London, EC1M 6BQ, UK.

We also acknowledge other consortium investigators of HALT PKD, CRISP and ADPKD Modifier: Drs. AB Chapman (University of Chicago), A Yu, and FT Winklhofer (Kansas Medical Center), KT Bae, KZ Abebe, and CG Patterson (University of Pittsburgh), GM Brosnahan and B Gitomer (University of Colorado Denver), WE Braun (Cleveland Clinic), FF Rahbari Oskoui (Emory University), PG Czarnecki (Brigham and Women's Hospital), FT Chebib (Mayo Clinic), D Miskulin (Tufts Medical Center, Boston), MF Flessner (NIDDK), DP Landsittel (University of Pittsburgh), WM Bennett (Legacy Health, Portland), Y Pei (University of Toronto), R Sandford (University of Cambridge), H Rennert (The Rogosin Institute, New York), Y Le Meur (Université de Brest), RT Gansevoort (University Medical Center Groningen), N Demoulin (Université Catholique de Louvain), and O Devuyst (University Hospital of Zürich).

Acknowledge other members of the Genkyst study: Drs. Le Meur Y, Grall A, Moal MC, Tanquerel T, Hanrotel C, Segalen I, Lanfranco L, Treguer L, Mesguen C, Kersale A, Capdeville A, Huynh V (Centre Hospitalier Universitaire, Brest); Hourmant M, Dantal J, Giral M, Meurette A, Lino M, Garandeau C, Hodemon-Corne B, Allain-Launay E, Cantarovich D, Blancho G, Hristea D, Couvrat G, Fakhouri F, Lavainne F, Vercel C, Chapal M, Le Fur A, Gourraud C, Deltombe C (Centre Hospitalier Universitaire, Nantes); Vigneau C, Morin MP, Le Pogamp P, Frouget T, Gie S, Rivalan J, Laruelle E, Richer C, Lorcy N, Golbin L, Terrasse M, Morice S, Brenier H, Michel A, Tomkiewicz E, Nguyen QL, Vabret E, Lavergne A, Pierre E, Chemouny J (Centre Hospitalier Universitaire, Rennes); Halimi JM, Longuet H, Gatault P, Merieau E, Barbet C, Buchler M, Golea G, Ghouti L, Gautard D, Sautenet B, François M, Fournier A, Baron C, Salmon C, Rabot N, Prat L, Valentin JF, Chevallier E, Birmele B, Genest C, Goin N, Goumard A (Centre Hospitalier Régional Universitaire, Tours); Bridoux F, Desport E, Thierry A, Ecotiere L, Touchard G, Belmouaz M, Javaugue V, Bauwens M, Fride-Leroy F, Bouteau I (Centre Hospitalier Universitaire, Poitiers); Subra JF, Augusto JF, Duveau A, Besson V, Cousin M, Sayegh J, Onno C, Maghakian MN, Demiselle J, Deschamps C, Garnier AS, Guibert F, Planchais M (Centre Hospitalier Universitaire, Angers); Charasse C, Stanescu C, Le Cacheux P, Baluta S, Leonetti F, Boulahrouz R, Ferrier ML, Freguin C, Simon A, Potier J, Coulibaly JM, Colombo, Delezire A (Centre Hospitalier Yves le Foll, Saint Brieuc); Renaudineau E, Dolley-Hitze T (Centre Hospitalier Broussais, Saint Malo) ; Perrichot R, Michez E, Mandart L, Menoyo V, Pincon E, Muresan C, Durand PY, Corlu L, Wegner I (Centre Hospitalier de Bretagne Atlantique, Vannes); Siohan P, Metes I, Guyon-Roger T, Wehbe B, Gueguen L, Drouet C, Loheac C (Centre Hospitalier de Cornouaille, Quimper); Sawadogo T, Le Guillou A, Le Jeune M, Beillard G, Lefevre S, Chamontin C, Georgescu S (Centre Hospitalier de Bretagne Sud, Lorient); Jousset P, Latif R, Massad M (Centre Hospitalier du Centre Bretagne, Pontivy); Jaulin JP, Couvrat G, Querard AH, Ottavioli JN, Target N, Chapal A, Le Fur A, Charpy V (Centre Hospitalier Départemental de Vendée, La Roche sur Yon); Besnier D, Regnier-Le Coz S, Blanpain A, Durault S, Larmet D, Le Clech A (Centre Hospitalier Georges Charpak, Saint-Nazaire); Pouteau LM (Centre Hospitalier de Laval); Labatut D (Centre Hospitalier Niort); Coindre JP, Sigogne M, Piccoli G (Centre Hospitalier Le Mans) ; Bachelet-Rousseau C, Delbes S, Fritz, O, Pourreau (Centre Hospitalier, La Rochelle) ; Mzoughi S (Centre Perharidy, Roscoff); Guillodo MP, Gosselin M, Depraetre P, Strullu B, Chaffara

E, Le Mee M (Association des Urémiques de Bretagne, Brest-Morlaix); Terki N, Goulesque K (Centre de Néphrologie et de Dialyse d'Armorique, Brest); Benarbia S, Dimulescu M, Rifaat M (Association des Urémiques de Bretagne, Quimper); Duneau G, Legrand D, Georges E (Association des Urémiques de Bretagne, Lorient); Seret G, Babinet F, Lanoiselee S (ECHO, Le Mans); Savoiu C, Testa A, Oancea I, Coupel I, Parahy S, Lefrancois G (ECHO, Nantes) ; Briand E, Bugnon D (ECHO les Sables d'Olonne

Acknowledge other members of the DIPAK consortium: Visser FW, Casteleijn NF, van Gastel MDA, Messchendorp AL, Neijenhuis MK, Pena MJ, Spithoven EM, Gansevoort RT (University Medical Center Groningen); D'Agnolo HMA, Lantinga MA, Gevers TJ, Wetzels JF, Drenth JPH (Radboud University Medical Center Nijmegen); Salih M, Zietse R (Erasmus Medical Center, Rotterdam); Losekoot M, Soonawala D, de Fijter JW (Leiden University Medical Center).